DOE/JPL-954521-77/3
DISTRIBUTION CATEGORY UC-63
IR-10016-1



# INTEGRAL GLASS ENCAPSULATION FOR SOLAR ARRAYS

P.R. YOUNGER
W.S. KREISMAN
A.R. KIRKPATRICK

THE WORK WAS PERFORMED FOR THE JET PROPULSION LABORATORY, CALIFORNIA INSTITUTE OF TECHNOLOGY UNDER NASA CONTRACT NAS7-100 FOR THE U.S. DEPARTMENT OF ENERGY, DIVISION OF SOLAR TECHNOLOGY

THE JPL LOW-COST SILICON SOLAR ARRAY PROJECT IS FUNDED BY DOE AND FORMS PART OF THE DOE PHOTOVOLTAIC CONVERSION PROGRAM TO INITIATE A MAJOR EFFORT TOWARD THE DEVELOPMENT OF LOW-COST SOLAR ARRAYS

INTERIM REPORT NUMBER 1
NOVEMBER 1977

PREPARED UNDER CONTRACT NO. 954521 FOR
JET PROPULSION LABORATORY
CALIFORNIA INSTITUTE OF TECHNOLOGY
PASADENA, CALIFORNIA 91103



spire
CORPORATION

This report contains information prepared by Spire Corporation under a JPL subcontract. Its content is not necessarily endorsed by the Jet Propulsion Laboratory, California Institute of Technology, the National Aeronautics and Space Administration or the Department of Energy.

DOE/JPL-954521-77/3
Distribution Category UC-63
IR-10046-1

# INTEGRAL GLASS ENCAPSULATION FOR SOLAR ARRAYS

Interim Report

Contract Number 954521

November 1977

Prepared for:

JET PROPULSION LABORATORY
California Institute of Technology
Pasadena, CA. 91103

Prepared by: Peter O. Young
Principal Investigator

Approved by: Allen R. Kirkpatrick
Program Manager

SPIRE CORPORATION
Patriots Park
Bedford, MA. 01730

TABLE OF CONTENTS

LIST OF ILLUSTRATIONS

LIST OF TABLES

## 1.0 INTRODUCTION

This report describes a fourteen month effort from May 1976 to July 1977 to develop integral glass encapsulation for solar cell arrays. Electrostatic bonding (ESB) has been used to join silicon solar cells to borosilicate glass without the aid of any organic binders or adhesives. The results of this investigation have been to demonstrate, without question, the feasibility of this process as an encapsulation technique. The potential of ESB for terrestrial solar arrays was clearly shown. The process is fast, reproducible, and produces a permanent bond between glass and silicon that is stronger than the silicon itself. Since this process is a glass sealing technique requiring no organics it makes moisture tight sealing of solar cells possible.

Electrostatic bonding is a process through which a variety of dissimilar materials may be permanently joined without the use of adhesives. With elevated temperature to produce ionic conductivity and an externally applied electric field to drive mobile ions, irreversible chemical bonds are formed at the interface of the pieces being joined. Metals, semiconductors and dielectrics can be joined to glass by this technique. For the present application, bare silicon solar cells or those with a variety of antireflective coatings may be joined to glass. Glass to glass sealing may be accomplished with the aid of an inorganic interfacial layer.

Glass offers many advantages as an encapsulation material. Existing solar cell module designs that incorporate glass require additional potting and sealing compounds to provide optical coupling between the glass

and cells, and to seal the module edges. Addition of these organic materials reduces the effectiveness of glass as an encapsulant. Only an all glass system will allow full advantage of this material to be taken. At the initiation of this program there existed no practical, cost effective technique for producing integral glass encapsulation of terrestrial solar cells. It was the goal of this program to demontrate that ESB could become such a technique. Prior to this effort, electrostatic bonding had been used for covering of spacecraft solar cells. However, in space environments radiation damage rather than weathering is the primary degradation mechanism to be protected against. Furthermore, spacecraft cells are smaller than terrestrial cells and the problems associated with size scale-up had not been solved. Bonding to the irregular surface presented by heavily metallized cells had not been demonstrated. Bonding to large areas where small thermal expansion mismatches would result in large residual stress had not been attempted. Aside from oxidation, the effects of atmosphere on bonding had not been assessed.

It was intended that Phase I of this program would be directed at these problems and would show that electrostatic bonding could be utilized in a cost effective manner to provide reliable long term glass encapsulation of terrestrial solar arrays. Feasibility of ESB for terrestrial solar cell encapsulation was clearly shown in Phase I of the program. Large area bonds can now be routinely made to heavily metallized cells with a variety of AR coatings. Major glass deformation (up to the full thickness of the solar cell) can now be accomplished during bonding. A controlled environment bonder has been constructed. This facility allows bonding of samples up

to eight inches square in a variety of atmospheres. Bonding can now be done without cell degradation due to oxidation. Bond strengths have been measured and found to be more than adequate for encapsulation purposes. Multiple cell demonstration modules have been fabricated without loss of cell performance caused by bonding.

# 2.0 ENCAPSULATION REVIEW

## 2.1 Encapsulation Requirements

The primary purpose of an encapsulation system for terrestrial solar arrays is to protect the component cells and interconnects from the effects of the ambient environment. In addition to weathering, certain random events, such as lightning, must be guarded against. Characteristics of a good encapsulation system include:

1. Moisture resistance.
2. Chemical stability.
3. UV stability.
4. Thermal stability.
5. Impact resistance.
6. Resistance against microorganisms.
7. High transmission of photons in the response band of the solar cell ($\approx$ 0.4-1.2 $\mu$m).
8. Effective optical coupling to the cells.
9. Insensitivity to dust deposits.
10. Fire resistance.

The relative importance of these factors depends on the local climate. It might be possible to vary the encapsulation system design to suit the environment but an ideal system would offer full protection against all factors. Since cost effectiveness is mandatory, a single universal system is desirable.

A large number of encapsulation systems and materials have been identified.[1] The degree to which the above list of requirements is met varies widely among the suggested materials. Since this report deals with a glass

encapsulation technique these other materials will not be discussed. The properties of glass make it a superior encapsulation material.

Glass is a unique material offering many advantages for solar cell protection. Some of the properties of glass that make it well suited to encapsulation include:

1. Excellent hermeticity.
2. Excellent chemical stability (water, acid, corrosion resistant).
3. Excellent weatherability including resistance to dust accumulation.
4. Optical compatibility with solar cells.
5. Expansion coefficient match to silicon (selected materials).
6. High thermal emissivity ($\varepsilon = 0.94$).
7. Good structural strength and stability.
8. Absence of toxic components.
9. Nonflamability.
10. High dielectric strength.
11. Routine production in large volume.
12. Low cost.
13. Adaptability to automated array assembly.
14. Compatibility with hybrid solar thermal-photovoltaic concepts.

Existing glass encapsulation systems vary in the extent to which they take advantage of these properties. When secondary encapsulants are used in conjunction with the glass many of the advantages are lessened. Full

advantage of the characteristics of glass can be had only with an integral encapsulation system. Methods of achieving integral glass encapsulation are considered in the next section.

## 2.2 Review of Non ESB Integral Encapsulation Techniques

Many developmental programs have been conducted over a number of years with objectives related to achieving satisfactory integral glass covers for spacecraft solar cells [2-11]. One task of this program was to survey the results of these earlier efforts for possible promise as terrestrial encapsulation methods. The methods considered were:

1. Electron beam evaporation
2. RF sputtering
3. Ion beam sputtering
4. Frit and fuse.

While it is conceivable that new development might lead to sufficient improvement of some method that it could be reconsidered, at present these techniques appear to be incapable of providing adequate terrestrial function. The first three, the molecular deposition methods, are inherently too expensive for meeting an encapsulation cost objective of the order of $\$1/ft^2$. Technically none of the approaches appears to have practical potential for terrestrial use. After substantial development efforts each resulted in highly stressed, thickness limited coatings which had poor or at best questionable survivability characteristics under thermal cycling and humidity. Alteration of requirements upon the cover material to reflect terrestrial rather than space environment would have little bearing upon the results unless very thin coatings ($<<25\ \mu m$) could be satisfactorily employed. A short summary of experience with each technique is given below:

Electron Beam Evaporation

The electron beam evaporation process was investigated primarily by Heliotek [2,3,4] for a number of years. High power electron beam guns were utilized to achieve glass deposition rates exceeding $10^{-2}$ μm/sec, by far the highest rates among the molecular deposition techniques. A number of glasses were tried for compatibility with this process. Best results were achieved with Corning type 1720 aluminosilicate glass which could be deposited to maximum thicknesses of less than 250 μm.

Covers deposited by electron beam evaporation were characterized by very high stress levels ($\geq 3 \times 10^8$ dynes/cm$^2$), serious darkening and appreciable yield losses. An additional problem of the process involved high temperatures (> 300°C) caused by radiated heat from the evaporating glass and a necessity to utilize approximately $10^{-4}$ torr of residual oxygen in the evaporation chamber to minimize darkening of the deposited glass due to suboxides. At these cell temperatures the background oxygen reacted with cell contact metal to cause contact failures or at least necessity for additional contact processing.

Heliotek environmental tests showed the electron beam evaporated covers consistently unable to withstand the effects of high temperatures and humidity without delamination. The covers did withstand thermal shock and thermal cycling and experienced only minor degradation due to ultraviolet exposure.

The electron beam evaporation process must be carried out in vacuum. Careful cell cleaning and preparation are required. Cost projections for space solar cells at production volume level were in the range of $0.50 - $0.80 per 2 x 2 cm cell at a cover thickness of 100 µm. The process is energy inefficient.

The electron beam evaporation process must be considered technically unsuccessful for deposition of integral glass more than approximately 50 µm thick and at best marginally acceptable for thinner films. The economics for terrestrial modules should be improved relative to the space cell cover projections but, as is thought to be the case with all of the molecular deposition processes, could probably never become feasible for $500 per peak kilowatt modules.

RF Sputtering

RF sputtering of integral glass covers was investigated in the late 1960's by Texas Instruments [5] and later more successfully by Electrical Research Association, England[6,7]. These efforts showed some technical promise for spacecraft cell covers. The Electrical Research Association development was performed using a 5 kW RF system which could coat a small area with Corning 7070 glass at a rate of slightly less than $10^{-3}$ µm/sec. No significant rate improvement was envisioned for a small scale production process as coating quality was rate dependent. Highly stressed ( ~3 x $10^7$ dynes/cm$^2$) type 7070 glass covers as thick as 300 µm were demonstrated. Cell temperature during cover deposition was maintained at 25°C. Good cover adhesion was observed and quality of the deposited 7070 glass was equivalent to that of the 7070

as supplied by Corning. Cells with RF sputtered 7070 covers exhibited reasonably good stability during environmental test.

The economics of the RF sputtering process are not promising. The necessity to employ very low deposition rates in an expensive evacuated facility leads to a costly coating. Electrical Research Association projected production volume costs for 200 μm thick covers onto 2 x 2 cm cells as over $1.00 per cell. Process energy consumption is substantial.

While the RF sputtering process could be used to deposit thin 7070 glass integral coatings which might be technically adequate for some encapsulation purposes, the economics of the process are poor.

Ion Beam Sputtering

Integral coatings of many glass materials deposited by high vacuum ion beam sputtering have been investigated by Ion Physics Corporation [8,9]. Best results were achieved with 7070 glass. Highly stressed ( ~1 x $10^8$ dynes/$cm^2$) coatings to thicker than 250 μm were deposited at a rate of approximately 3 x $10^{-4}$ μm/sec. The process employed a high current beam of high energy argon ions as the sputtering source. Projected deposition rate in a production facility remained below $10^{-2}$ μm/sec.

Covers exhibited good physical and optical characteristics. Good environmental stability of cover material was demonstrated but was not maintained if the facility

was operated on an irregular basis. In this case a susceptibility of covers to delamination due to humidity exposure was observed.

Ion Physics projected production volume cost for 250 μm thick 7070 covers as approximately $0.50 per 2 x 2 cm cell. Due to the low deposition rate which is inherent with the ion beam sputtering process and because of the expensive required facility, it is unlikely that this cost could be much reduced for very large volume terrestrial module situations. Energy consumption of the process is high.

As in the case of RF sputtering, ion beam sputtering might be technically adequate for deposition of very thin encapsulating films of 7070 glass, but costs would be excessive.

Frit and Fuse Methods

Attempts to deposit integral covers by "frit and fuse" techniques were made by Hoffman Electronics in the early 1960's[10] and later by General Electric[11]. In this approach a glass suspension slurry is applied to the cell surface and then is fused to the cell in a high temperature furnace. The best results achieved were by GE using specially developed glasses which could be fused to cell surfaces at a temperature of 520° C for 18 minutes. Maximum coatings thickness was less than 100 μm and solar cell output degradation was generally observed. Achieved coating quality and environmental stability of the coatings were relatively poor.

The frit and fuse technique is simple, relatively fast and energy efficient. Expensive and complex facilities are not required. If the process could be technically adequate, production level economics might be attractive. However, technical performance possibilities are doubtful.

## 2.3 ELECTROSTATIC BONDING TECHNOLOGY

This section will deal with the electrostatic bonding process. The mechanics of the process will be described. The advantages of this technique for integral glass encapsulation will be discussed along with the requirements on the glass material. A discussion of the status of the technology at the initiation of the program will follow.

To electrostatically bond a solar cell to a sheet of glass, the cell and glass must be heated to a temperature above 400°C. At this point thermal dissociation of alkali oxides takes place within the glass and the glass exhibits ionic conductivity. A high voltage is applied across the sample. The cathode, connected to the glass, draws positive ions of sodium, lithium or potassium away from the cell/glass interface. This ion depletion causes a polarization layer to develop at the points of contact along the interface. At adjacent locations where the surfaces are not in contact an electrostatic field is produced which acts across the gap to force the surfaces together. Thus, for surfaces that nearly match, a bond may begin at a few isolated spots and propagate across the entire interface. The degree to which unmatched surfaces will join depends upon temperature. At high temperature,

the glass is sufficiently plastic that the electric field causes it to deform around minor irregularities such as cell contacts. Since the electrostatic force is proportional to the square of the reciprocal of the surface separation, major irregularities on sharp objects cannot be deformed around with only the field action. Application of external pressure can be useful in this situation.

When the cell and glass surfaces are in intimate contact, oxygen ions move under the influence of the field through the glass to the silicon where chemical bonding occurs. Once complete, the bond is permanent and its strength exceeds that of both the silicon and glass.

The electrostatic bonding process, as described above, offers many advantages for solar cell encapsulation. The process is inherently simple, fast, reproducible and energy efficient. The resulting bonds are strong, virtually stress free and stable. The equipment required is neither elaborate nor expensive to produce. Potential for automation is high, with adaptation to in-line processing straightforward.

In order to use electrostatic bonding for solar cell encapsulation and take full advantage of the available features, certain requirements on the glass must be met. These include thermal expansion coefficient match to silicon, high optical transmission, low viscosity at bonding temperature and good resistance to weathering.

Matching of the thermal expansion coefficients of silicon and the glass is a dominant consideration in glass selection. The choice of available materials was

immediately limited (by this consideration) to Corning 7070 and 7740 glasses. The rationale leading to the choice of 7070 will be described in more detail in Section 4.3.

Prior to this program no attempts had been made to adapt electrostatic bonding to terrestrial solar cell encapsulation. The potential for this application was clear from the work on spacecraft cells done under an earlier Air Force program. The status of ESB technology that existed before this terrestrial cell encapsulation program started is described in the final report of the Air Force contract.[12] Much of the earlier program was devoted to design and construction of an automated bonder, development of bonding techniques for a variety of spacecraft cells and analyzing radiation resistance of ESB covered cells. While this experience was valuable in directing the present program it must be said that little was known as to how the process would be adaptable to terrestrial cell encapsulation. The simplicity, and reproducibility of the process had been demonstrated. Bonding to polished silicon up to 2 cm square had been done routinely and the strength and performance of the bond was well established. In addition to silicon, bonding to antireflective coatings of $SiO_x$ and $Ta_2O_5$ had been demonstrated.

Serious problems, each with a bearing on terrestrial cell bonding, remained. Major deformation bonding had not been accomplished. Problems of bonding around heavy contact metallization had not been solved. Large area ( > 2 cm x 2 cm) bonding had not been tried. Glass surface requirements had not been assessed. All cover slips for spacecraft cells had polished surfaces. Evaluation of

pressed or rolled glasses had not been made. It was known that ambient atmosphere caused severe cell degradation during bonding due to contact oxidation. However, no further study of the effect of bonding environment had been made. These and other not yet determined problems existed at the start of the present program.

## 3.0 PROGRAM PLAN

### 3.1 Program Goals

The purpose of this program was to assess the feasibility of electrostatic bonding as an encapsulation technique for terrestrial solar arrays. To accomplish this goal it was necessary to extend the existing spacecraft cell covering technology and to make adaptations to that technology as dictated by the special needs of terrestrial photovoltaic systems. A demonstration of the applicability of ESB as an encapsulation technique required several major developments. Equipment capable of bonding large area, multiple cell samples had to be constructed. In addition to the mechanical handling problems associated with large samples, the facility had to operate under a controlled environment so that cells could be bonded and interconnected without loss of performance due to contact degradation effects.

An assessment of existing glass materials had to be made. On the basis of thermal expansion match to silicon the primary glass had to be selected. The surface requirements for this glass had to be evaluated. Conditions for major plastic deformation of this material had to be established. Associated with this last task were problems of adhesion of the glass to the bonding electrode surface.

An extension of the range of bondable materials had to be made. Metallization systems compatible with high temperature processing had to be established for both cell contacts and interconnections. Metal forms, such as vacuum evaporated thin films, screen processed thick films, electroplated layers and solid ribbons, had to be

evaluated. Bonding of anti-reflective coatings had to be demonstrated along with bonding of dielectric materials that could be used for glass-to-glass sealing. Techniques for handling these materials in the various available forms had to be developed.

Both existing technology and extended range technology had to be critically evaluated if electrostatic bonding was to be convincingly demonstrated. Thus test methods had to be established so that bond strength, reliability and integrity could be proven.

The combination of all the above efforts then had to lead to the fabrication of a series of demonstration modules. These functioning, multi-cell structures would have to show that the basic configuration of a large array system could be produced using electrostatic bonding. These demonstration modules had to show that cells could be bonded and interconnected with no loss in performance caused by the ESB process. Finally, these modules had to be tested to show that they could withstand the effects of environmental exposure.

The next section will discuss technical approach. The scope of this program was not wide enough to allow full evaluation of each system, technique or material upon which experiments were performed. The approach was to develop basic processes that would demonstrate the feasibility of ESB and to identify promising methods that warranted further development.

## 4.0 TECHNICAL DISCUSSION

### 4.1 General

This section will deal with the various technical aspects of the program including:

1. Fabrication of an interim and a controlled environment bonder.
2. Glass studies including materials selection, evaluation of polished, rolled, pressed and ground surfaces, and pressing experiments.
3. Metallization studies including evaporated films, screen processed films, ribbons, foils and meshes.
4. Bond quality evaluation through lap shear and hermeticity testing.
5. Module development and production.

### 4.2 Design and Construction of Electrostatic Bonders

During this program two electrostatic bonders were constructed. The first, or interim, bonder was assembled for the purpose of assessing design requirements for a controlled environment, large area bonder. Since large area and major deformation bonding had not previously been demonstrated it was necessary to determine the range of bonding parameters required for these applications. Accordingly, the interim unit was made large enough to handle six inch square sheets of glass. This bonder was capable of all functions necessary for the mechanical development of glass encapsulated solar cell modules. However, since it operated in ambient atmosphere, bonding of cells without serious loss in performance was not possible.

During the first six months of the program the interim bonder was also used to develop bonding techniques applicable to solar cell encapsulation. These included major deformation bonding around contact metallization patterns, gross plastic deformation of the glass around complete cells, bond quality evaluation, and experimental evaluation of glass types and surface finishes.

At the middle of the program the controlled environment bonder became operational. A diagram of the bonder assembly appears in Figure 1, with a photograph of a completed facility appearing in Figure 2. The process chamber is composed of two parts: a loading region and a bonding region. The loading area consists of an access door, sample transfer mechanism and feed table with water cooling capability. The bonding region has two identical 10 inch square heating plates. These heaters have radiation shields and water cooling to reduce chamber heating. The lower heater is isolated from electrical ground so that it may serve as the high voltage electrode. The upper heater assembly may be raised or lowered by a hydraulic motion mechanism. This drive system is coupled to the upper heater plate by a ball and socket joint which allows the plate to pivot and thus conform to samples of uneven thickness. Alternately, this ball and socket joint can be locked in place to insure parallelism of the two heater plate surfaces.

Samples are loaded into the bonder through the access door. A flow of gas through the chamber maintains a nonoxidizing atmosphere when the door is open. While the sample rests on the feed table, the system is evacuated to a pressure of 10 microns or less. A gas manifold allows backfilling with any of four gasses.

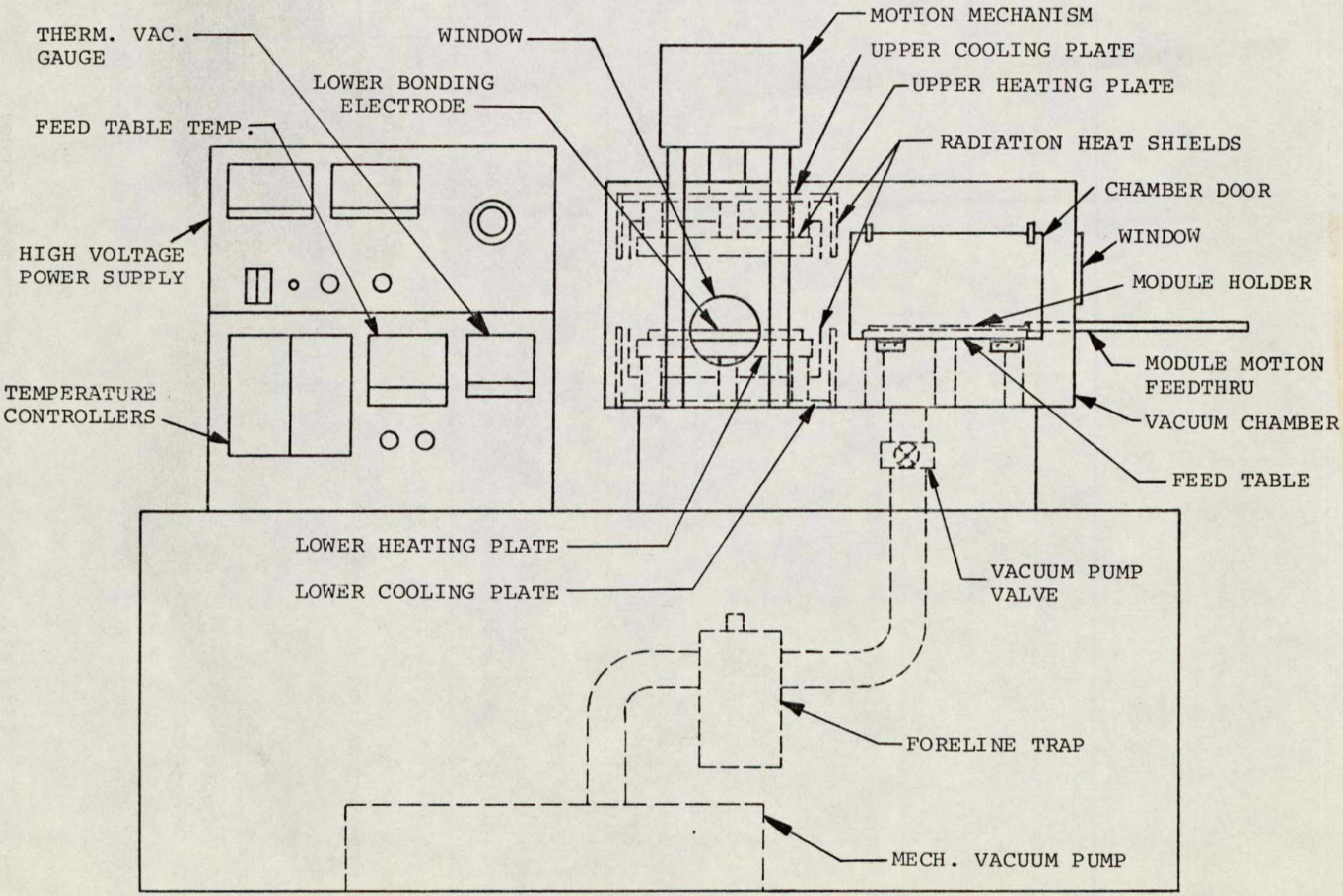


Figure 1. Controlled Environment Bonder Schematic

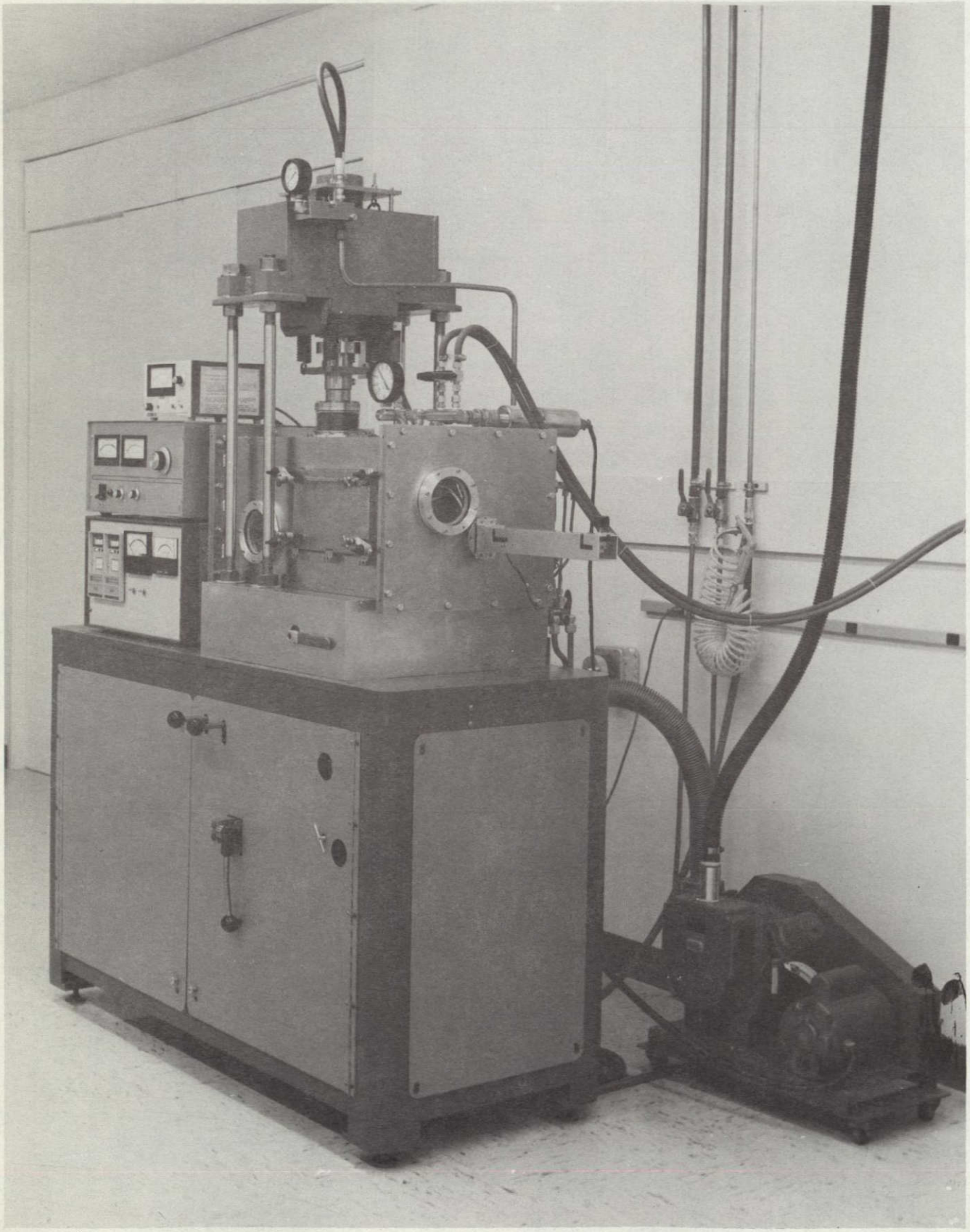

Figure 2. The Controlled Environment Bonder

These gasses may be nitrogen, helium, argon or forming gas (95% $N_2$, 5% $H_2$). Bonding may be done under vacuum. When the proper bonding environment has been obtained the sample is transferred from the loading region to the surface of the bottom heater plate. The top heater is brought down to contact the sample from above. After a short preheat, a high voltage between 500 and 1000 VDC is turned on. A current of a few $mA/cm^2$ is passed for a period of about three minutes. This current rises at first as the sample temperature rises and the polarization layer is established and then falls. A thorough investigation of bond dynamics has not been conducted but it is felt that the bond is formed by the time that the current begins to drop. Immediately after the voltage is turned off, the upper heater is raised and the sample is withdrawn to the feed table. Water cooling of this table reduces sample temperature rapidly so that the piece can be removed from the chamber within a few minutes.

Total process time is approximately 30 minutes. However, most of this time is consumed in loading, pumpdown, backfill, cooling and unloading. Figure 3 shows the time temperature profile of a typical sample as it goes through bonding and cool down. Since the actual process time is on the order of five minutes, throughput would be high for in-line processing.

System performance has been satisfactory although some components did require modification. Bonding of large area samples was immediately possible. Figure 4 shows one of the first samples to be produced in the controlled environment bonder. It consists of five 2 1/4 inch diameter cells bonded to a single sheet of 7070

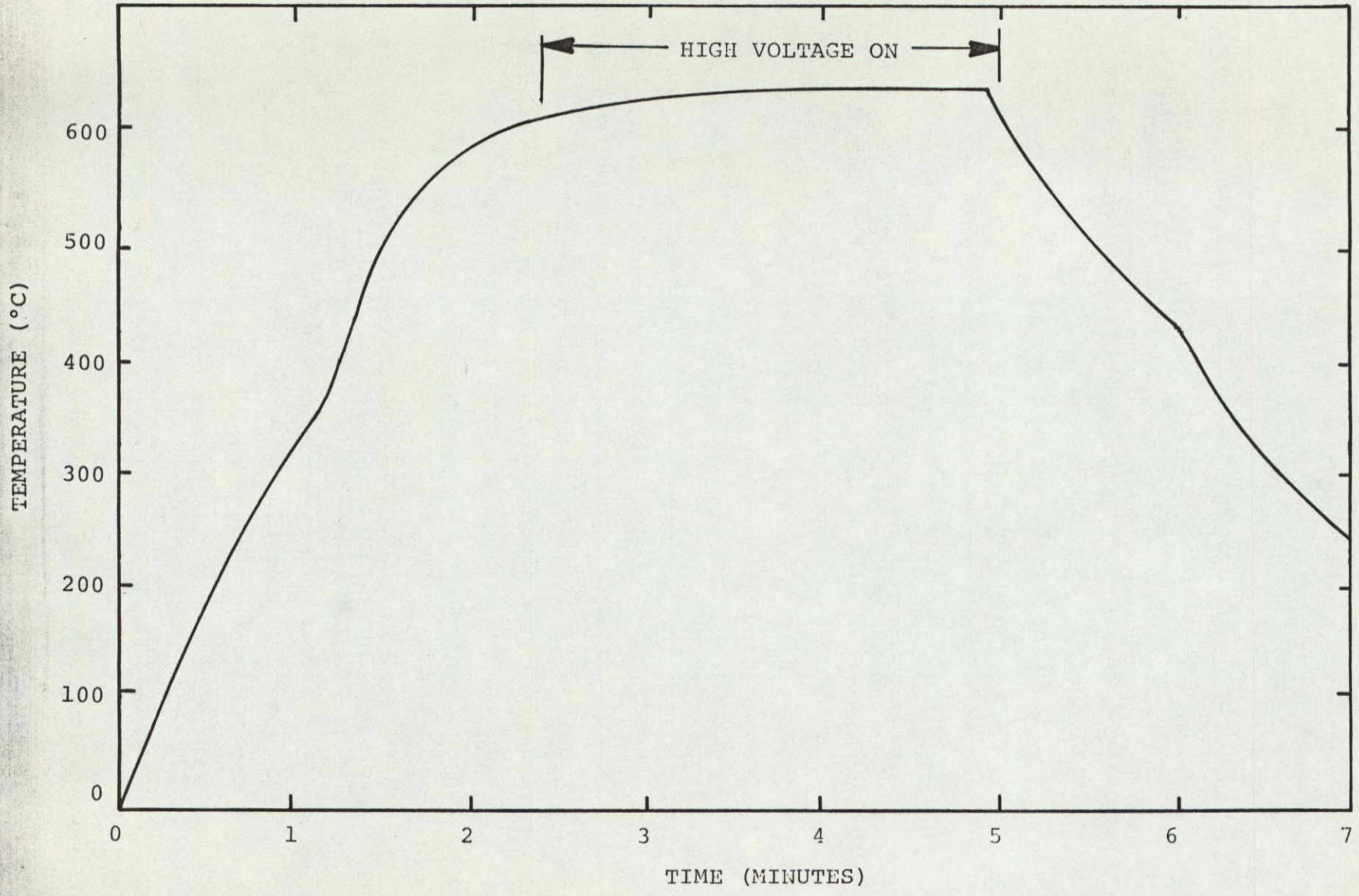


Figure 3. Time-Temperature Profile of a Typical Sample

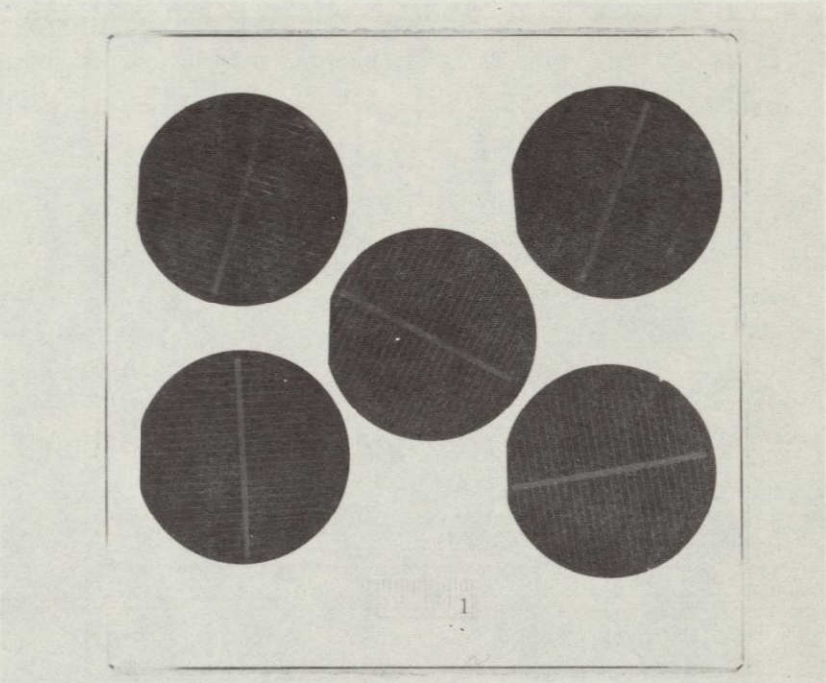

Figure 4. Five 2 1/4 Inch Diameter Solar Cells Electrostatically Bonded to a Single Sheet of 7070 Glass

glass. The first demonstration of simultaneous bonding of a multiple cell configuration showed the potential of electrostatic bonding for terrestrial solar cell encapsulation.

## 4.3 Glass Studies

Both theoretical and experimental investigations of glass materials have been made. First, evaluations of the physical properties of several glasses, considered for electrostatic bonding of silicon solar cells, were made in order to select the best available material. Tests were conducted to determine the requirements for the glass surface. Polished, rolled, pressed, and ground glass surfaces were studied. Glass pressing was also investigated.

As mentioned, there are several properties of the glasses that determine their applicability to the ESB process. These parameters are listed below in approximate order of relative importance.

| Parameter | Requirement |
|---|---|
| 1. Expansion Coefficient | Close match to silicon. |
| 2. Optical Transmission | Should be clear over .4 - 1.2 μm |
| 3. Viscosity/temperature characteristic | Prefer annealing point as low as possible. |
| 4. Weathering resistance | No loss of transmission due to environmental exposure. |

Among commercial formulations available from Corning Glass Works, the following borosilicate candidates were considered:

| Code | Expansion Coefficient $^{o}C^{-1}$ (0-300°C) | Color | Annealing Point (°C) | Weathering Resistance |
|---|---|---|---|---|
| 7740 | $33 \times 10^{-7}$ | Clear | 560 | Excellent |
| 7070 | $32 \times 10^{-7}$ | Clear | 496 | Fair |
| 9741 | $40 \times 10^{-7}$ | Clear | 450 | Probably Inadequate |

Code 7070 glass had been used in previous electrostatic bonding efforts because of its excellent thermal expansion match to silicon. The other glasses, 7740, and 9741, were considered because other properties made them attractive. Pyrex (7740) glass has excellent weatherability and is commercially available in rolled sheet form. Currently, sheet 7070 glass is available only in pressed squares. These are usually ground and polished to make them ready for bonding. Code 9741 glass offers a lower annealing point than the other materials and thus would be the easiest to plastically deform.

Appendix I shows properties of these candidate glasses in more detail. It is clear from the thermal expansion data that 9741 glass is not well matched to silicon at high temperature. Because of the divergence of the two expansion curves, 9741 glass was dropped from consideration.

To assess the applicability of 7740 glass, a stress analysis was conducted. The difference in expansion coefficients of silicon and 7740 glass results in a high stress concentration around the rim of the bonded cells.

The 7740 glass has a lower expansion coefficient than silicon. After the rigid electrostatic bond is formed and the materials are returned to room temprature, the silicon tries to contract more than the glass. As a result, the silicon is left under tension and the bonded glass under compression. However, at the outer edge of the silicon, the glass which is being compressed interfaces with free glass not bonded to silicon. The effect is to try to decrease the diameter of the interface which causes the unbonded glass at the interface to be put into radial tension and tangential compression. The peak tensile stress right at the outer edge of the silicon wafer is estimated to be in the range 3500 to 4000 psi (see Appendix 2 for details of the calculation). This stress level approaches the yield strength of the glass and when augmented by additional thermal or mechanical stress, causes the interface to fail.

Figure 5 shows a typical crack pattern that develops in bonded silicon/7740 samples after thermal cycling. The sample shown underwent several cycles from liquid nitrogen temperature to 100$^{o}$C. The additional thermally induced stresses combined with those present after bonding to cause failure. This effect is not seen if 7070 glass is used in place of the 7740 material.

If silicon and 7070 glass are bonded at 490$^{o}$C there should be no residual stress because the net thermal expansions match at that temperature. In practice, bonding is usually performed at somewhat higher temperatures, but the residual stress is still small.

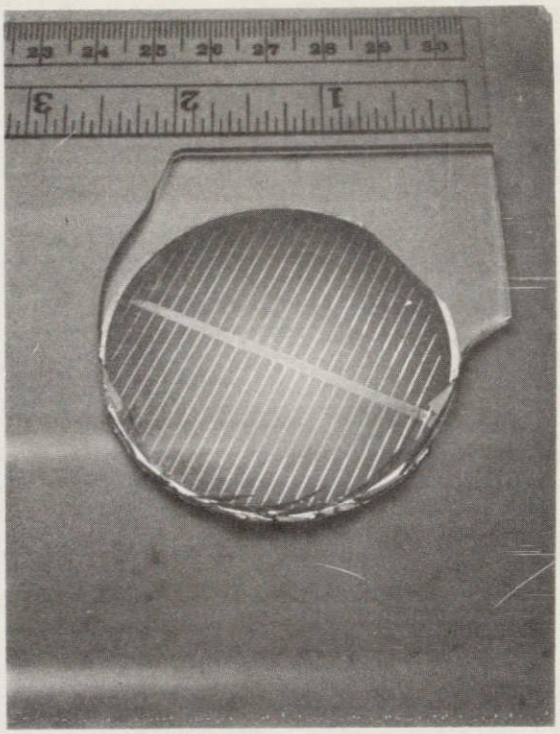

Figure 5. Typical Crack Pattern Occurring with 7740 Glass

Thus 7070 was used throughout this program as the primary glass material. Use of this glass for electrostatic bonding will continue until a formulation with as good expansion coefficient match to silicon, but lower annealing point is developed.

The surface condition of sheet glass varies considerably with the method of preparation. Pyrex glass is available in rolled sheet with minor surface irregularities and in a form that approaches a polished condition. Sheet 7070 glass is currently made only by casting, a process which leaves very large surface irregularities. These pressed sheets of 7070 glass are ground flat and polished before using.

Several tests were made to determine the glass surface requirements for bonding. Polished glass is ideal but the surface of rolled glass also proved adequate in all tests. The rolled glass was flat and with only very minor irregularities. This type of finish results from a continuous melt process. Less automated rolling processes might produce unacceptable surface irregularities.

The two surfaces of pressed glass are noticibly different. One side of a pressed glass blank is relativity smooth with occasional irregularities caused by the bottom of the mold. The other side has surface discontinuities as large as .02 inch. It was possible to bond cells to either of these surfaces but extreme care was needed to avoid cracking of the silicon. The surface of pressed glass is not considered acceptable for routine bonding.

Ground glass presents a much different set of requirements than the rather smoothly varying surface of pressed or rolled glass. In this case, the surface irregularities are very sharp. Attempts were made to bond polished silicon to flat glasses with 70, 45 and 14 micron finishes. No bonds could be formed. The surfaces could not be brought together by the electrostatic forces because those forces fall off rapidly with distance. It is possible to bond to ground glass surfaces if the temperature is raised to a point where the glass will flow easily during the bond. The surface is then reformed and no longer has a ground finish.

The table below summarizes the studies on glass surface. Rolled 7070, from a continuous melt facility should offer no problems for encapsulation by electrostatic bonding.

Table I
Summary of Glass Surface Evaluation

| Glass Surface | Applicability to ESB |
|---|---|
| Polished | Ideal but expensive to prepare. |
| Rolled | Fully acceptable |
| Pressed | Bonds with difficulty probably not acceptable |
| Ground | Bonds only with surface reforming - not acceptable. |

## 4.4 Metallization Studies

Three forms of metallization systems were investigated during this program. These were evaporated films, screen processed thick films and preforms such as ribbons, foils, and mesh. Since they were most compatible with standard solar cell processing and mechanically easiest to handle, evaporated films were studied first.

Several restrictions govern the use of evaporated films as cell interconnects and electrical feedthroughs. The metal must be compatible with silicon (no low temperature eutectics and low diffusion rate), have low contact resistance to silicon and low sheet resistance, be able to form electrostatic bonds and exhibit good adhesion to glass.

At the beginning of this program, three materials were considered for use in ESB modules. The restriction to silver, aluminum and silicon was based solely on past experience and lack of knowledge of the performance of other substances in electrostatic bonding. It was originally proposed to make solar modules with evaporated films serving cell interconnects, electrical feedthroughs, and interfacial bonding layers. The properties of these materials as they apply to module use are listed below.

| Material | Advantages | Disadvantages |
|---|---|---|
| Silicon | Easily evaporated; compatible with cell; readily bonded | High electrical resistivity-must be alloyed to become a good conductor. |
| Aluminum | Easily evaporated; high electrical conductivity | Forms eutectic with silicon at 577°C. |
| Silver | High electrical conductivity | Requires base layer to get good adhesion to glass; ability to form electrostatic bonds in question. |

While all three materials have certain advantages that make them attractive candidate materials, not one could be used alone to make electrical connections from cell to module exterior. For this reason, other metals were considered. These high temperature metals were tantalum, molybdenum, chromium, and titanium. Tests of the bondability and electrical properties of thin evaporated films of these materials were to be made to evaluate their applicability to use in solar modules.

Films of these metals, vapor deposited onto 7740 glass, were bonded to bare pieces of 7740 glass. Hand pull tests and thermal cycling between room and liquid nitrogen temperatures showed that all materials formed electrostatic bonds. A more quantitive measure of their performance was obtained by measuring the strength of the bonds under shear forces. Details and results of these tests are described in Section 4.5 below.

Measurements of the electrical properties of the thin films presented some development problems. It was originally intended to measure contact resistance between the films and bare silicon. However, high sheet resistance of the films made such measurements meaningless. This high resistivity was due either to the structural nature of the films or to the formation of oxides within the films.

In order to develop thin film metallization techniques with these materials it would have been necessary to make a through study of the evaporative process and post evaporative sintering of each material. Since such an investigation was not directly related to nor essential to the development of electrostatic bonding technology, it was not undertaken. Further experiments were conducted with materials of proven applicability, primarily the standard cell metallization system of titanium/silver.

One test of thin film metallization evaluated the integrity of the film under glass deformation. Terrestrial solar cells have contact metallizations with thickness of 1 mil or more. Cell interconnections consisting of thin films would have to withstand the glass deformation required to accomodate the surface irregularities presented by these contacts. Advanced module concepts calling for

much greater glass deformation would further strain thin film interconnections.

One quarter-inch wide strips of metal consisting of five microns of silver over a thin layer of titanium were deposited onto sheets of 7070 glass. Rectangles of bare silicon crossing these strips were then bonded to the glass as shown in Figure 6. The edge profile of the silicon produced by scribing and breaking was the sharpest that would be encountered with bonded cells. The change in the film resistance after bonding was measured as a function of deformation. For deformations up to 0.007 inch, no significant change in film resistance was measured. See Table II. Greater deformation (up to 0.017 inch) caused the film to stretch and increase in resistance although continuity was never lost. The conclusion to be drawn from this experiment is that evaporated film interconnections can be used under all but the most severe conditions of deformation bonding.

Fully functioning cells have been bonded to 7070 glass with vapor deposited Ti/Ag films serving as interconnection metallization. The I-V curve of such a bonded cell, Figure 7, shows there is no loss in electrical output caused by bonding. The use of thin film interconnections will be discussed in more detail in Section 4.6.

Screen processing is an attractive alternative to vacuum deposition of metallization systems. This technique is already used in production for application of cell contact patterns since it is faster and less expensive than evaporation. Even greater economic

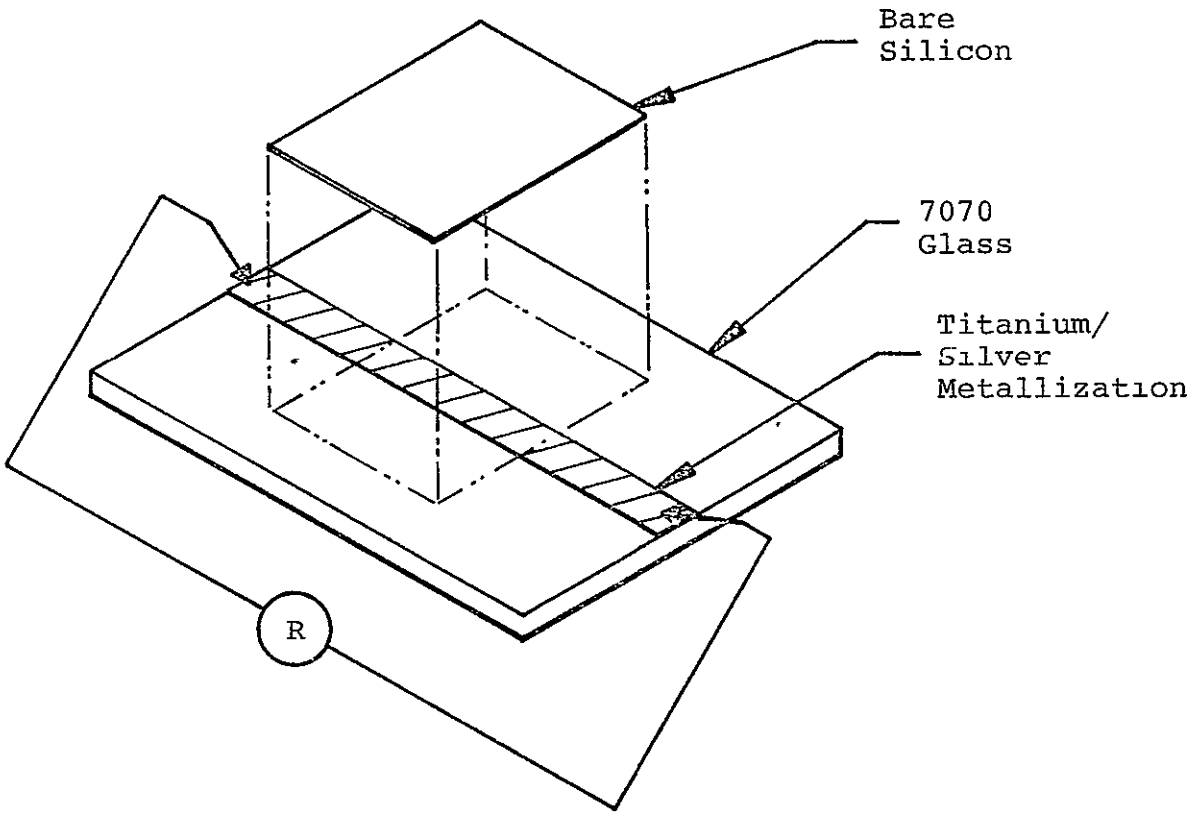


Figure 6. Configuration for Deformation Bonding Test

TABLE II

Silver Film Resistance
Before and After Deformation Bonding

| Depth of Glass Deformation (inches) | Film Resistance Before Bond (milliohms) | After Bond (milliohms) |
|---|---|---|
| 0.004 | 15 | 15 |
| 0.006 | 15 | 35* |
| 0.007 | 28 | 29 |
| 0.009 | 15 | 29 |
| 0.017 | 28 | 230† |

* Glass cracked during bond

† Silicon cracked during bond

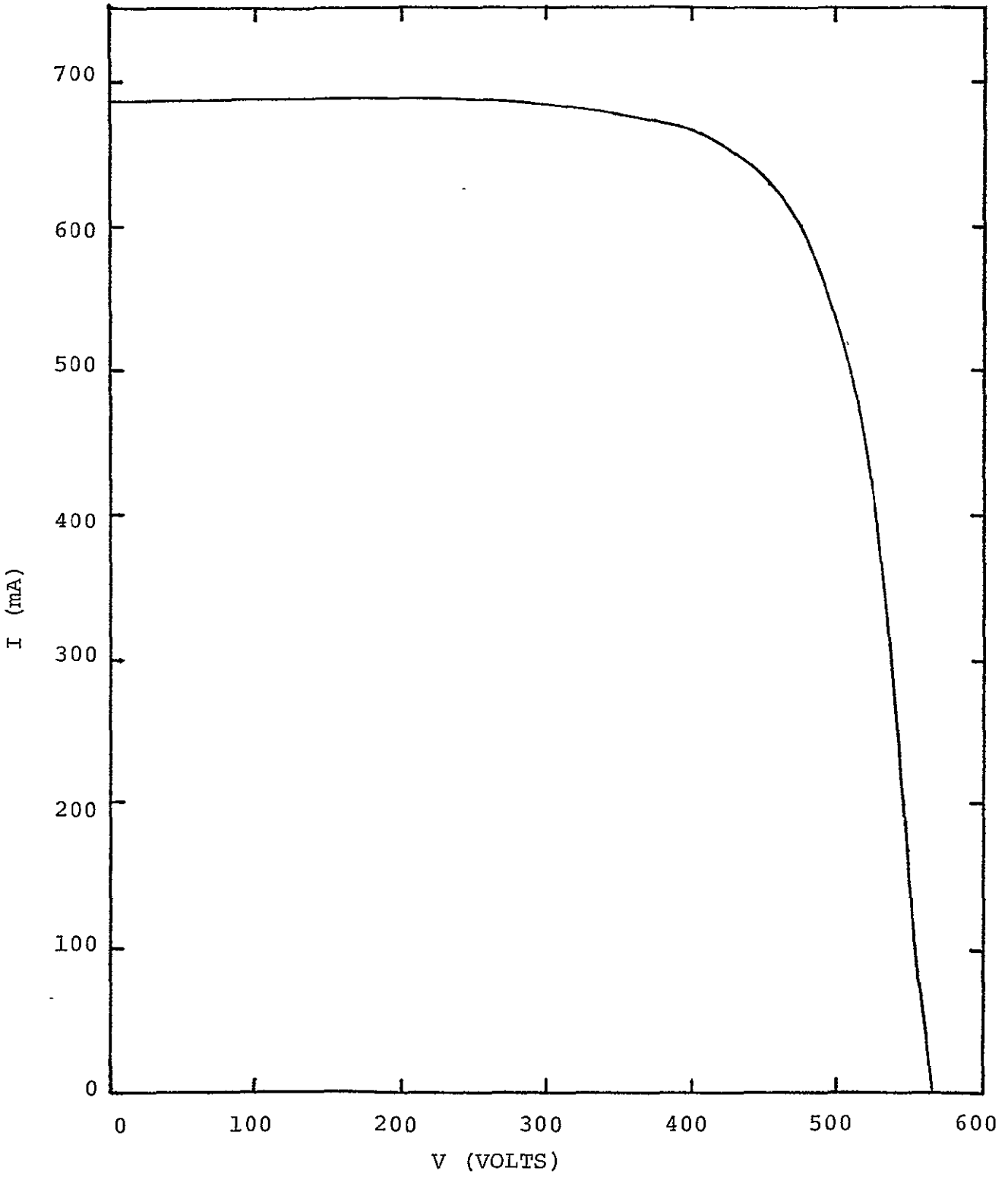


Figure 7. AMO I-V Curve of an Electrostatically Bonded Terrestrial Solar Cell

advantage could be realized if the complete cell contact and interconnection pattern for an entire multiple cell array were screened onto a single sheet of glass in one operation.

The primary problems associated with bonding bare cells to pre-metallized glass is achieving low contact resistance betwen the silicon and the metallization. Low contact resistance is achieved with unmetallized cells by appropriately adjusting the firing schedule. For contacts screened onto the glass interaction between the cells and the metal can be achieved during the bonding cycle, but the flexibility of the bonding cycle is limited. Working within the confines of the bonding cycle, good contact to the cell must be achieved by variation in the both metal and glass content of the screening ink.

Some preliminary results were obtained with screened silver. A conventional pattern for a 2 1/4 inch diameter cell was printed onto 7070 glass using silver ink with a glass frit content of 10%. An unmetallized cell was then bonded to the glass. The electrical output of this cell, Figure 8, is seriously limited by high contact resistance between the silicon and the metal and is degraded by shunting occuring at the cell edge. This shunting results from the metal deforming around the cell edge during bonding. This problem also occurs with thin film metallization.

A solution to shunting, caused by metallization crossing the cell edge, was found in the pattern of Figure 9. This pattern was developed for use in four cell demonstration modules using thin films, and will be discussed in more detail below.

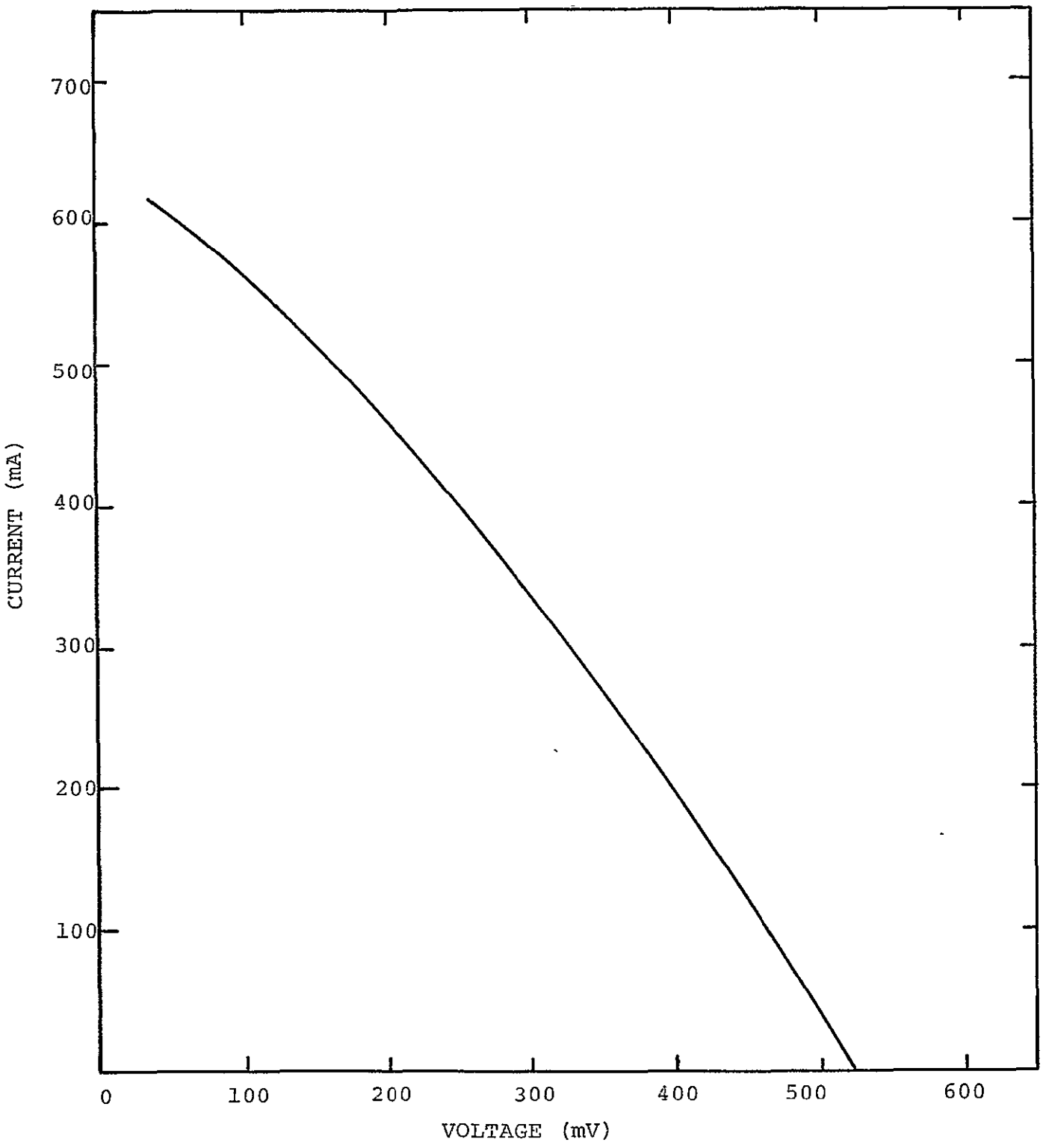


Figure 8. I-V Curve of Unmetallized Cell Bonded to 7070 Glass with Screen Printed Metallization

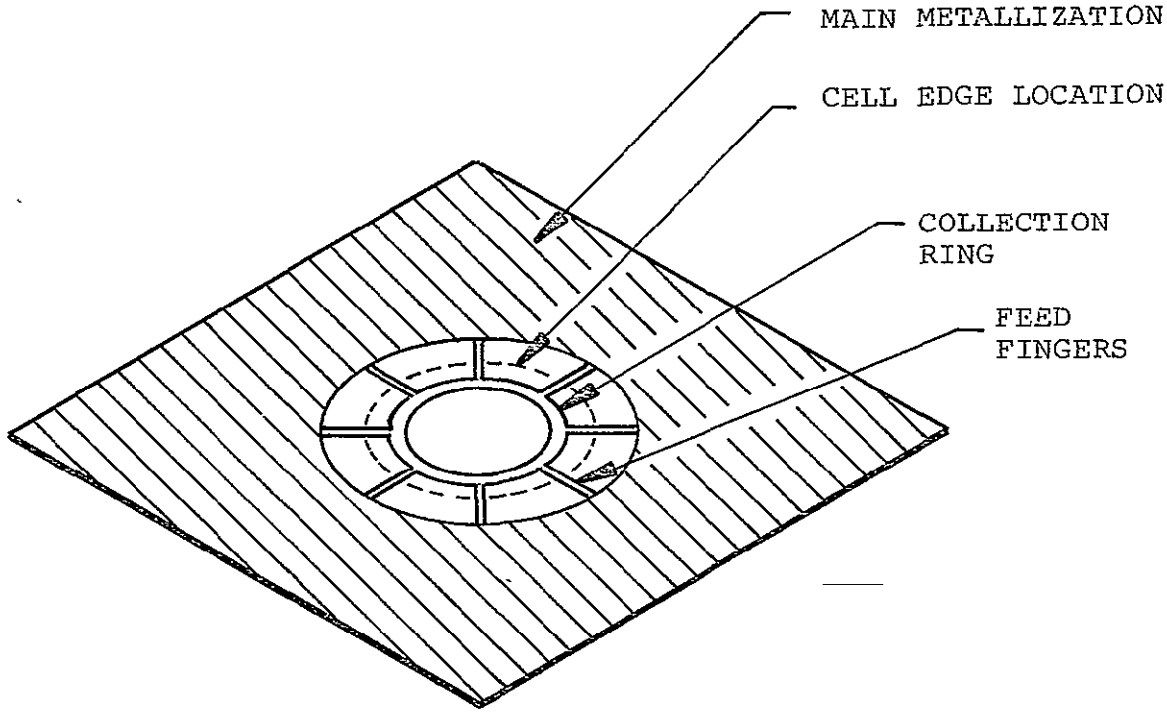


Figure 9. Interconnection Pattern for Screened Processed Metallization

A screen printed interconnect pattern of this configuration was used to bring current out from a conventionally metallized cell that had been bonded to a printed sheet of 7070 glass. The I-V curve, Figure 10, shows that shunting remains a problem, probably due to the thickness of the printed metal. A dielectric ink overprint or mechanical insulator would be needed to eliminate shunting.

Solar module output terminals require a durable material to withstand weathering and mechanical stresses. Evaporated films would not be adequate for this purpose but bonded metal foils might function quite well.

Kovar, since it is used in conventional glass sealing to certain borosilicate glasses, was tried. Attempts were made to bond 0.010 inch Kovar to 7070 and 7740 glasses at 550°C. No permanent bonds could be formed although temporary adhesion was strong enough to cause large divot fracturing in the glass. Apparently electrostatic bonds did form, but failure occured upon returning the sample to room temprature. The thermal expansion of Kovar is more than twice that of the two glasses between room and bonding temperatures. Thinner foils (~ 0.001 inch) might perform better, especially if the bonding temperature was lowered.

Other foils that were tested included copper, aluminum, tantalum, titanium, and molybedenum. Bonding of all but copper had been demonstrated in thin film form but of these five materials only aluminum could be bonded in foil form. Thickness, expansion mismatch, and surface condition of the foils may well have contributed to failure. The behavior of aluminum is some what surprising

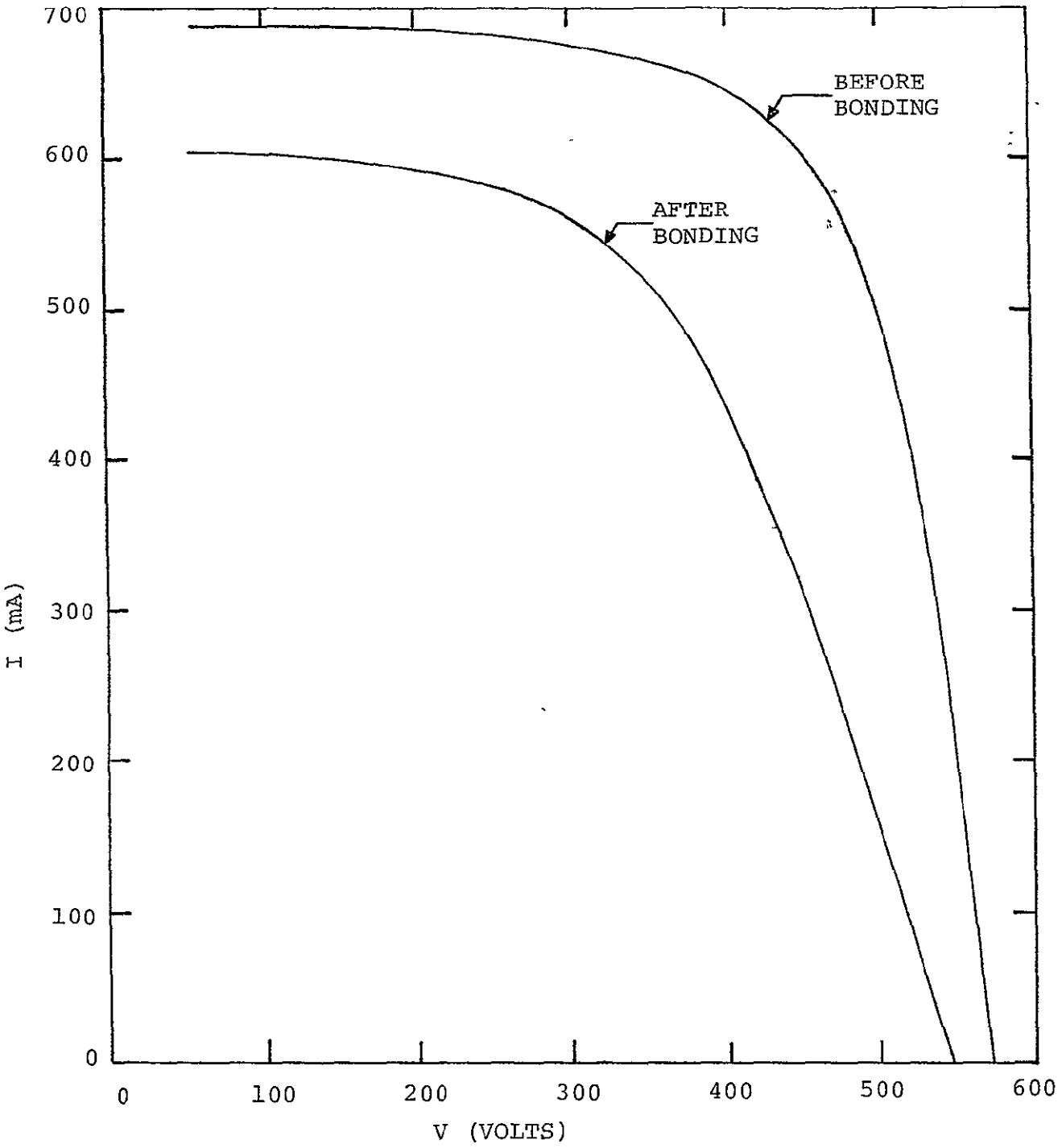


Figure 10. AMO I-V Curve of Cell Bonded to Screened Metallization Pattern of Figure 9

since its thermal expansion coefficient ( 27 x $10^{-6}$ /°C, 20-300°C) is very large compared to 7070 (3.2 x $10^{-6}$/°C, 0-300°C). The high ductility of the metal may explain why bonds between aluminum and 7070 do not fail.

The successful bonding of large area aluminum foils suggested that this material could be used for cell interconnections. Figure 11 shows a 2 1/4 inch diameter cell with conventional titanium/silver metallization bonded to a piece of 7070 glass. Bonded to the glass, and extending under the cell edge is a sheet of 0.001 inch aluminum foil. Cell output suffers from severe shunting (See Figure 12) at the end of the contact bar. This effect is similar to what occured with screened metallization that extended beyond the cell edge. Methods to prevent this shunting were devised after this test and if used would probably greatly improve cell output.

## 4.5 Bond Quality Evaluation

Since a properly formed electrostatic bond will not fail under normal handling it was necessary to develop a method to evaluate bond integrity. One such measure of bond quality is the shear strength of bonded films. Measurements of this type were made at JPL on a number of samples.

The test configuration is shown in Figure 13. Two overlapping rectangles of 7740 glass were bonded together with the aid of an interfacial film applied by vacuum evaporation. Overlap area was approximately one half square inch. Preliminary tests, done under a variety of atmospheres, demonstrated the formation of bonds with aluminum, chromium, molybdenum, tantalum and titanium.

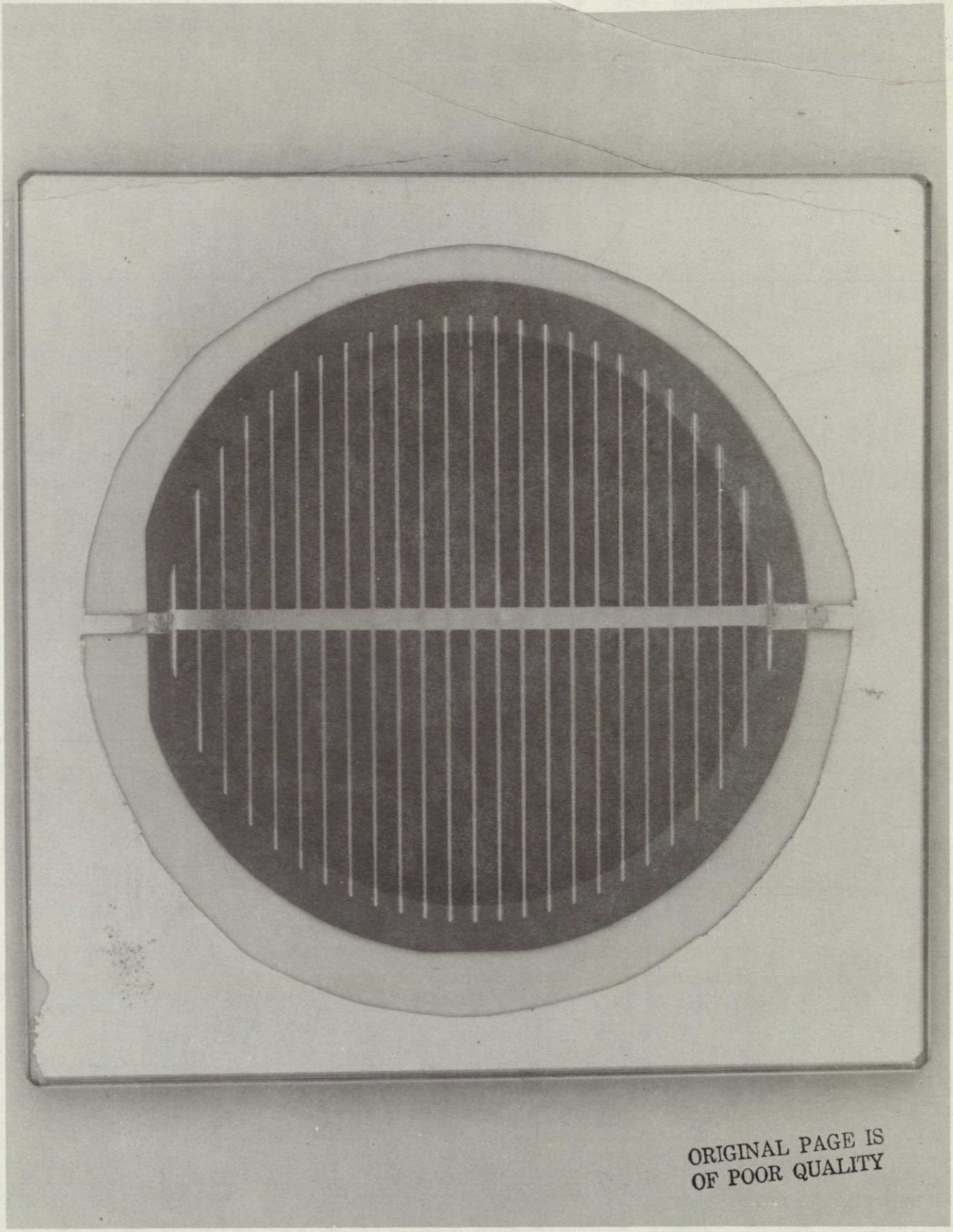


Figure 11. 2 1/4" Diameter Cell Bonded to a Piece of 7070 Glass with Bonded Aluminum Foil Metallization

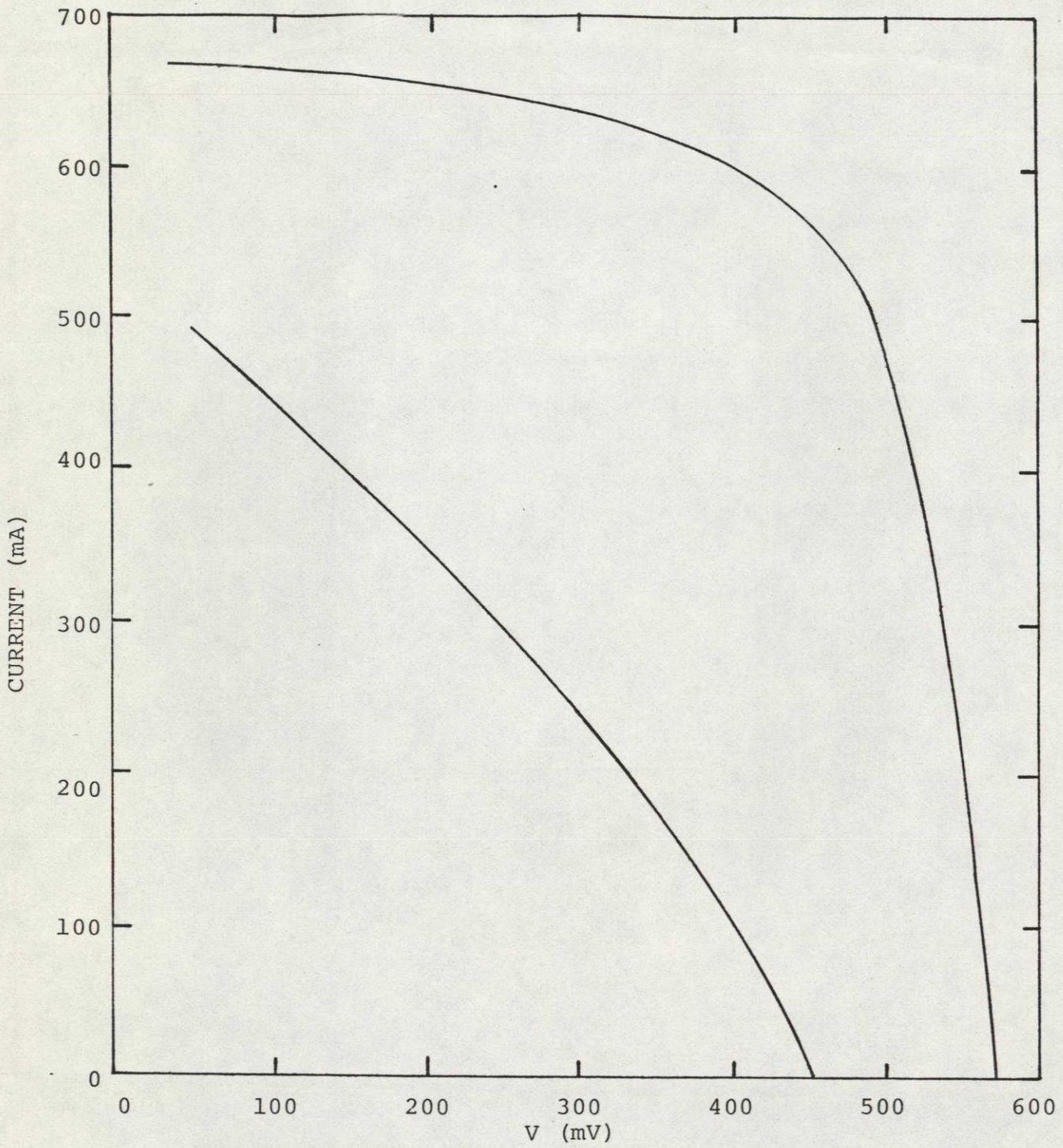


Figure 12. AMO I-V Curve of Cell Before and After Bonding to Glass with Bonded Aluminum Foil Metallization

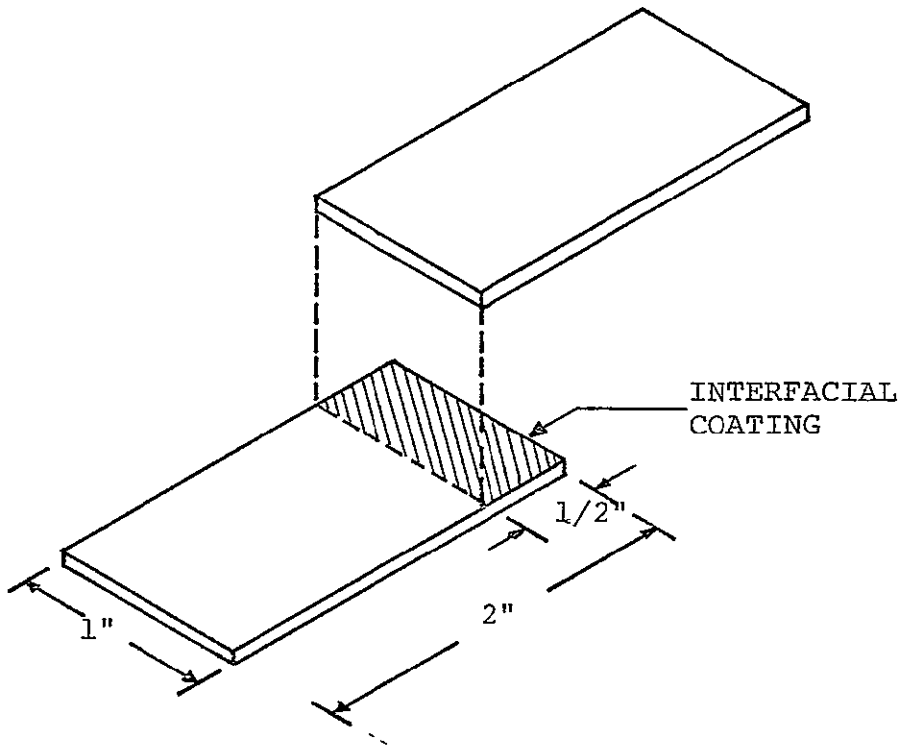


Figure 13. Configuration for Shear Strength Testing

Bonding was performed in atmospheres of nitrogen, forming gas and under vacuum. Bonding in argon atmosphere proved difficult due to the initiation of a glow discharge at bonding potentials of only a few hundred volts.

A systematic survey of bonds made under nitrogen was conducted. Evaporated films, 1000 Å thick were applied to sheets of polished 7740 glass. Each material was deposited in a single evaporation so that sample uniformity would be assured. Table III summarizes the results of this test series. In many cases, only a lower bound could be established for shear strength. This limitation was due to failures in the glass. Breakage of glass occured anywhere between 1000 and 2000 pounds of applied force. Thus variation is reported failure points, over 2000 psi, is due to slight differences in the glass mounting or strength and not the bond quality.

The total failures of molybdenum and silicon monoxide are surprising. Thermal cycling and hand pull tests had been performed on representative samples of each type and did not indicate potential failures. Molybdenum bond failures are also inconsistent with preliminary results obtained when the test capability was being established. An examination of other available samples with molybdenum interfaces prepared previously showed bonds could be separated. Thus it appears that bonds with these interfaces were weaker than first thought or their long term stability is poor.

TABLE III

Results of Lap Shear Tests Done on Samples
with Evaporated Film Interfaces

| Interface Material | Sample Number | Bond Result (% Bond) | Shear Strength at Failure (PSI) Individual | Average | Failure Mode |
|---|---|---|---|---|---|
| Al | 142A | 100 | 4000 | | |
| | 142B | 100 | 2500 | 2890 | Glass failure |
| | 154A | 100 | 2250 | | |
| | 154B | 100 | 2800 | | |
| Cr | 141A | 100 | 3600 | | Glass failure |
| | 141B | 80 | 1630 | | Bond shear |
| | 155A | 100 | 200 | 1780 | Bond shear |
| | 155B | 60 | 1670 | | Bond shear |
| M | 135 | 50 | 0 | | Bond fell apart |
| | 152A | 75 | 0 | 0 | upon loading into |
| | 152B | 80 | 0 | | test assembly |
| Si | 151A | 55 | 1250 | | Bond shear |
| | 151B | 70 | 1200 | 1390 | Bond shear |
| | 176B | 80 | 1710 | | Glass failure |
| SiOx | 144A | 60 | 0 | | Bond fell apart |
| | 144B | 70 | 0 | 0 | upon loading into |
| | 195A | 100 | 0 | | test assembly |
| Ta | 143A | 60 | 2000 | | |
| | 175A | 100 | 2940 | 2530 | Glass failure |
| | 175B | 98 | 3600 | | |
| Ti | 136A | 100 | 1580 | | Bond shear |
| | 153A | 55 | - | 2360 | Sample broken |
| | 153B | 100 | 3130 | | Glass failure |

The strongest bonds were formed with aluminum and tantalum. Titanium comes next but there is a large difference between the two samples tested. Chromium bonds were generally strong with one exception. The weak chromium bond sample is probably traceable to some irregularity in the bond conditions and might be discounted. Silicon bonds showed the greatest consistency. These test results should be considered preliminary. Not enough samples of any one type were prepared to give statistically meaningful results. Only one bonding atmosphere was involved. Others, such as vacuum, forming gas and helium should be evaluated. However, a working test configuration has been established. For the present, shear strengths up to 2000 psi can be measured. This limit is sufficient to identify weak bonds. The test range might be extended to evaluate bonds of such materials as aluminum and to compare bond strength to evaporated film adhesion. Determination of the best bonding atmosphere is also possible. An important practical consideration is the determination of the lowest shear strength that is acceptable for applications in solar cell encapsulation. Establishment of such a criterion would allow a broader choice of materials than would be possible if only maximum bond strength were considered.

Another series of test samples consisted entirely of screen processed films. Metallic or dielectric inks mixed with a small amount of glass frit were screened onto 7740 glass. After firing to drive off organic binders, the samples were bonded to another piece of glass. The

failure strengths, shown in Table IV, are only estimates because the true bonded area is frequently difficult to determine. The thick film may look bonded even though there is only adhesion due to fusion of the glass frit. Bond strengths may be in error by a factor of two due to this uncertainty. Nevertheless, the following general conclusions may be made: copper, and ground silicon did not form acceptable bonds; silica seal 1126 and silver appear to make strong bonds; silica seal 1141 is questionable; and finally silver must be fired at 600°C If the bond is to be acceptable.

A method for testing the hermeticity of glass encapsulated systems has been developed. Figure 14 shows the test configuration consisting of two glass sheets, one with a 0.06 inch deep recess in the middle. The 1/4 inch wide perimeter around this cavity is covered with an interfacial coating which acts as the bonding medium. After bonding the sample is put into a helium filled pressure vessel so that the interior can be filled with gas if a leak is present. Next, the sample goes into an evacuated bell jar connected to a mass spectrometer leak detector where the presence of helium would indicate a non-hermetic seal.

Cavities fabricated by sand blasting 7740 glass had widely varying depths and proved very delicate. One such sample, bonded under vacuum, imploded upon exposure to atmospheric pressure indicating that the bonded aluminum seal was tight. A second set of samples was prepared by milling cavities in 7070 glass. Those samples proved much stronger than the first. No test data have been received at this time, but a workable configuration has been established.

TABLE IV

Screen Processed Lap Shear Samples

| Sample # | Material | Firing Temp °C | Failure Strength (PSI) | Comments |
|---|---|---|---|---|
| 196(A) | Silica Seal 1141 | 500 | - | Broken - no adhesion |
| 196(B) | Silica Seal 1141 | 500 | 680 | |
| 235(A) | Cu | --- | 1170 | |
| 236(A) | Cu | --- | - | Broken - no adhesion; fired during bond cycle |
| 236(B) | Cu | --- | - | |
| 236(C) | Cu | --- | - | |
| 237(A) | Cu | --- | <140 | |
| 237(B) | Cu | --- | 470 | |
| 238(A) | Silica Seal 1126 | 550 | 1300 | ✓ |
| 238(B) | Silica Seal 1126 | 550 | 2600 | |
| 239 | Ag | 600 | 1800 | + |
| 240(A) | Ag | 600 | 2600 | + |
| 240(B) | Ag | 600 | 4400 | + ✓ |
| 240(C) | Ag | 600 | 3800 | + |
| 242(A) | Ag | 600 | 3100 | + |
| 242(B) | Ag | 600 | 2700 | + |
| 242(C) | Ag | 600 | 3100 | + |
| 243(B) | Silica Seal 1141 | 500 | - | Broken no adhesion |
| 244(A) | Silica Seal 1141 | 500 | - | Broken no adhesion |
| 244(B) | Silica Seal 1141 | 500 | 1060 | |
| 245(A) | Silica Seal 1126 | 550 | 2700 | + |
| 245(B) | Silica Seal 1126 | 550 | 1500 | |

Table IV (Continued)

| Sample # | Material | Firing Temp °C | Failure Strength (PSI) | Comments |
|---|---|---|---|---|
| 250(A) | Ag | 400 | 1460 | |
| 250(B) | Ag | 400 | - | √ Broken no adhesion |
| 250(C) | Ag | 400 | 1380 | √ |
| 251(A) | Ag | 400 | 890 | √ |
| 251(B) | Ag | 400 | 3030 | √ |
| 251(C) | Ag | 400 | 2980 | √ |
| 253(A) | ground Si | 600 | - | Broken no adhesion |
| 253(B) | ground Si | 600 | - | Broken no adhesion |
| 253(C) | ground Si | 600 | - | Broken no adhesion |

Two ground Si failed during sawing

√ Bonded interface failed

+ Glass failed

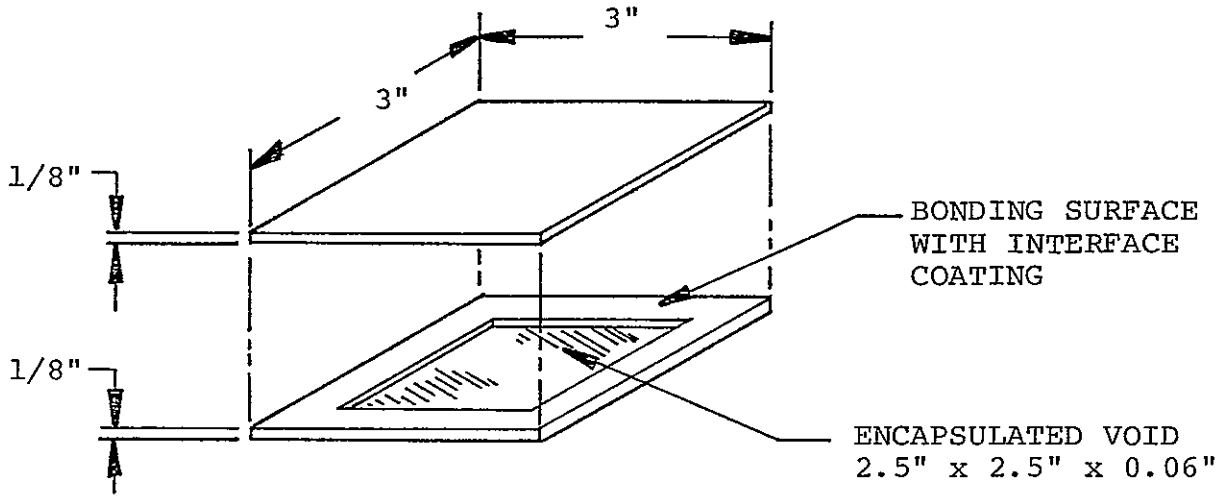


Figure 14. Hermeticity Test Specimen

## 4.6 Module Development

Three series of demonstration modules have been developed durng this program. These were intended to demonstrate the feasibility of ESB and provide functioning samples for environmental testing. Each of the three designs incorporates more advanced and more practical bonding procedures and techniques. Thus the first series (Type I) consists of integral front modules. Four cells are bonded to a single sheet of glass. Evaporated films bring power out from the fronts of bonded cells while soldered interconnects join the cells. An organic backing protects the cells, films and interconnects. This module is intended to demonstrate that functioning modules can be fabricated with electrostatic bonding techniques.

The second series, or Type II modules, demonstrates total glass encapsulation. These semi-integral modules have welded metal ribbons interconnecting the cells. A recessed back glass is bonded to the front glass through an interfacial silicon layer.

Type III modules are fully integral. They are identical to Type II modules with the exception that the two glass sheets are completely deformed around the cells. This design represents the most advanced module type since it offers complete cell protection and can be easily fabricated in a production bonder designed especially for it.

Figure 15 shows a Type I module. Evaporated films of titanium/silver cover the glass surrounding each 2 1/4 inch diameter cell, and carry the current from the cell fronts. Isolation of the four cells allows series

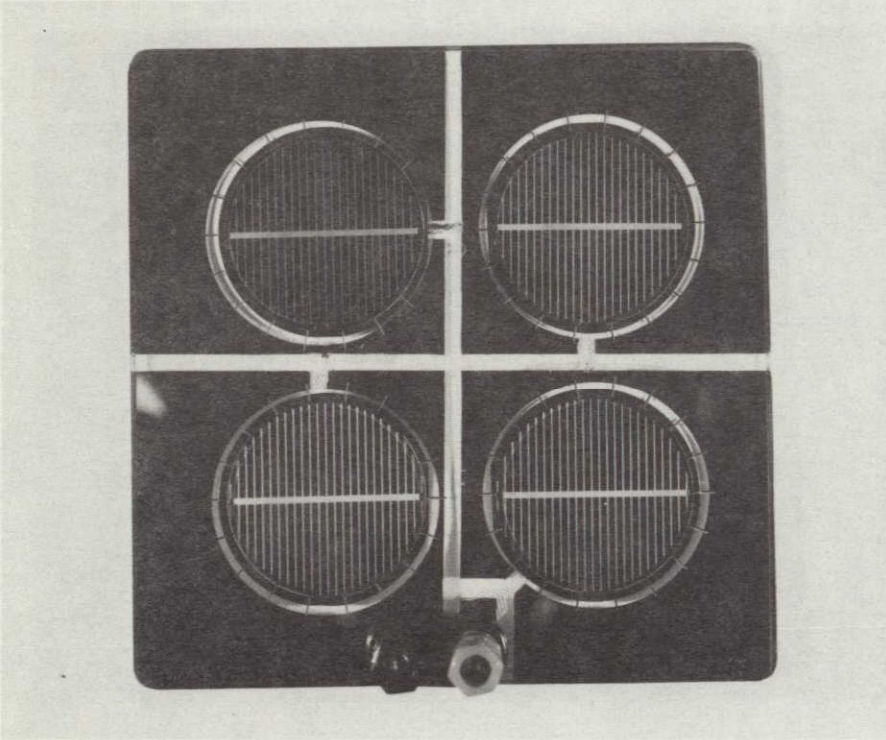

Figure 15. Four Cell Series Module Type I

interconnection by silver meshes soldered between the back of each cell and the front film metallization of the adjacent cell. Output termination is via standard binding posts attached through holes drilled in the glass. The back of this single glass sheet module is protected by an organic coating, either an RTV sealant or an asphalt/butyl rubber compound.

This design was not meant to represent a practical configuration for large scale solar arrays. No attempts were made to optimize the cell packing density nor is an organic back coating considered a viable candidate material for 20 year encapsulation. However, this design does demonstrate the feasibility of the process and provides test samples.

Shunting problems were encountered during initial attempts to fabricate modules of this design. Metallized glass was prepared with holes in the evaporated films that were just smaller in diameter than the cells. The continuous metallization extending under the cell was designed to pick up the current from the front contact fingers. However, as the glass was deformed around the cell contact fingers the evaporated film metallization also wrapped around the cell edge and shorted the junction.

The shunting problem was eliminated by reducing to a few percent the fraction of the cell edge crossed by metallization. The pattern shown earlier in Figure 9 provides a collection ring to pick up current from the cell contacts. The current is then fed out beyond the cell edge, to the main metallization, by a series of fine radial fingers. Since the fingers traverse only a few percent of the cell circumference shunting is negligible.

Four modules of this type were delivered to JPL for evaluation and testing. The I-V curves of these modules appear in Figures 16-19, while a summary of modules characteristics is given in Table V. The effect of electrostatic bonding on cell performance may be judged from the data of Table VI. Here the four cells of module M1008 are characterized before bonding and compared to the completed module. Such a comparison shows the following:

$V_{oc}$ (module) = 97% of sum $V_{oc}$ (cells)
$I_{sc}$ (module) = 91% of average $I_{sc}$ (cells)
$P_{max}$ (module) = 91% of sum $P_{max}$ (cells)
Fill Factor (module) = 99% of average of cells

The metallization pattern applied to the glass obscures an extra 10% of the cell area. Correction for this lost incident energy gives:

$I_{sc}$ (module) = 101% of average $I_{sc}$ (cells)
$P_{max}$ (module) = 97% of sum of $P_{max}$ (cells).

Thus for cells of this quality, electrostatic bonding causes minimal degradation of electrical performance.

Since evaporated films on glass are neither practical nor cost effective and since organic coatings do not offer cell protection approaching that provided by

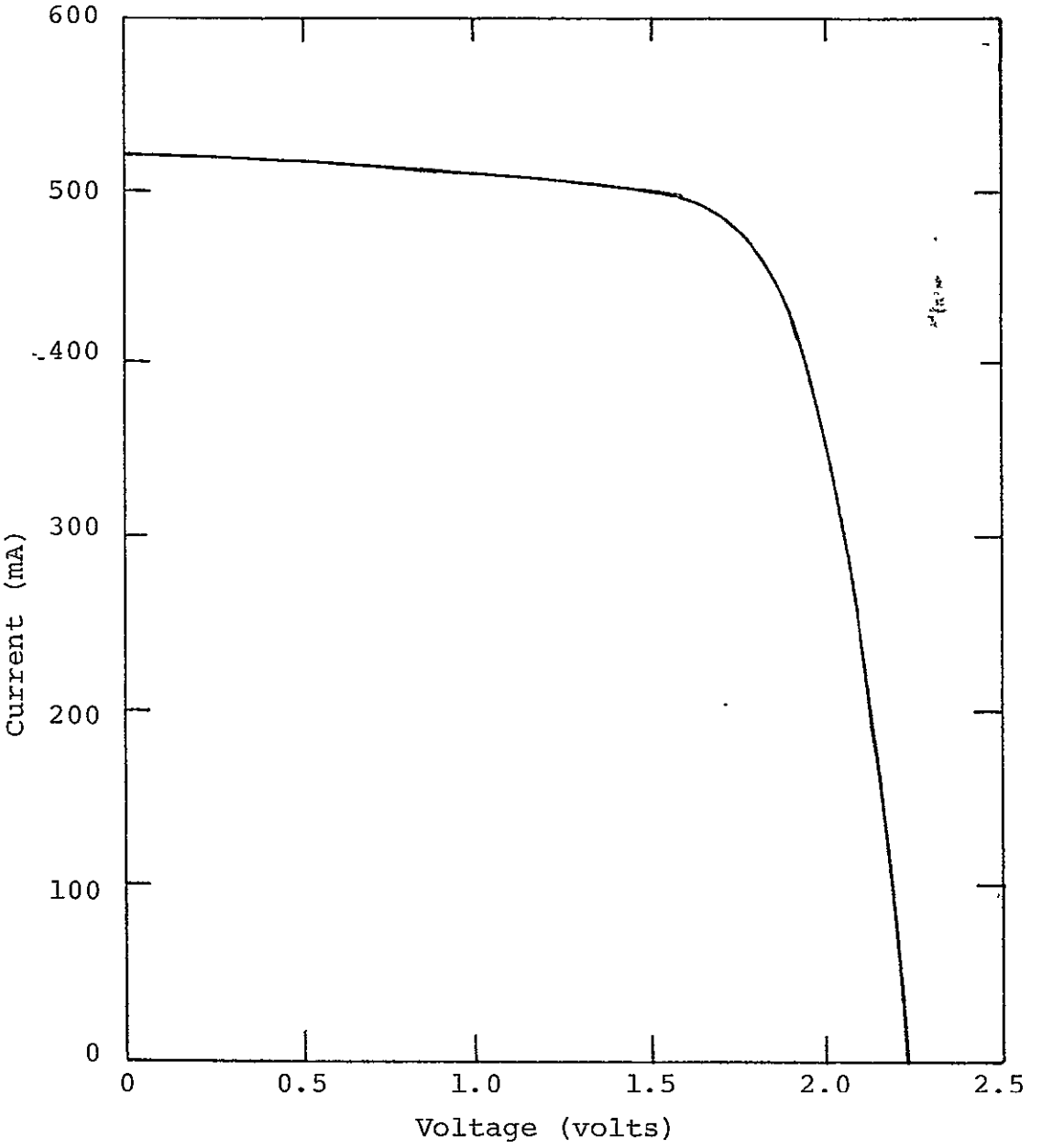


Figure 16. AMO I-V Curve of Four Cell Electrostatically Bonded Module, M1008

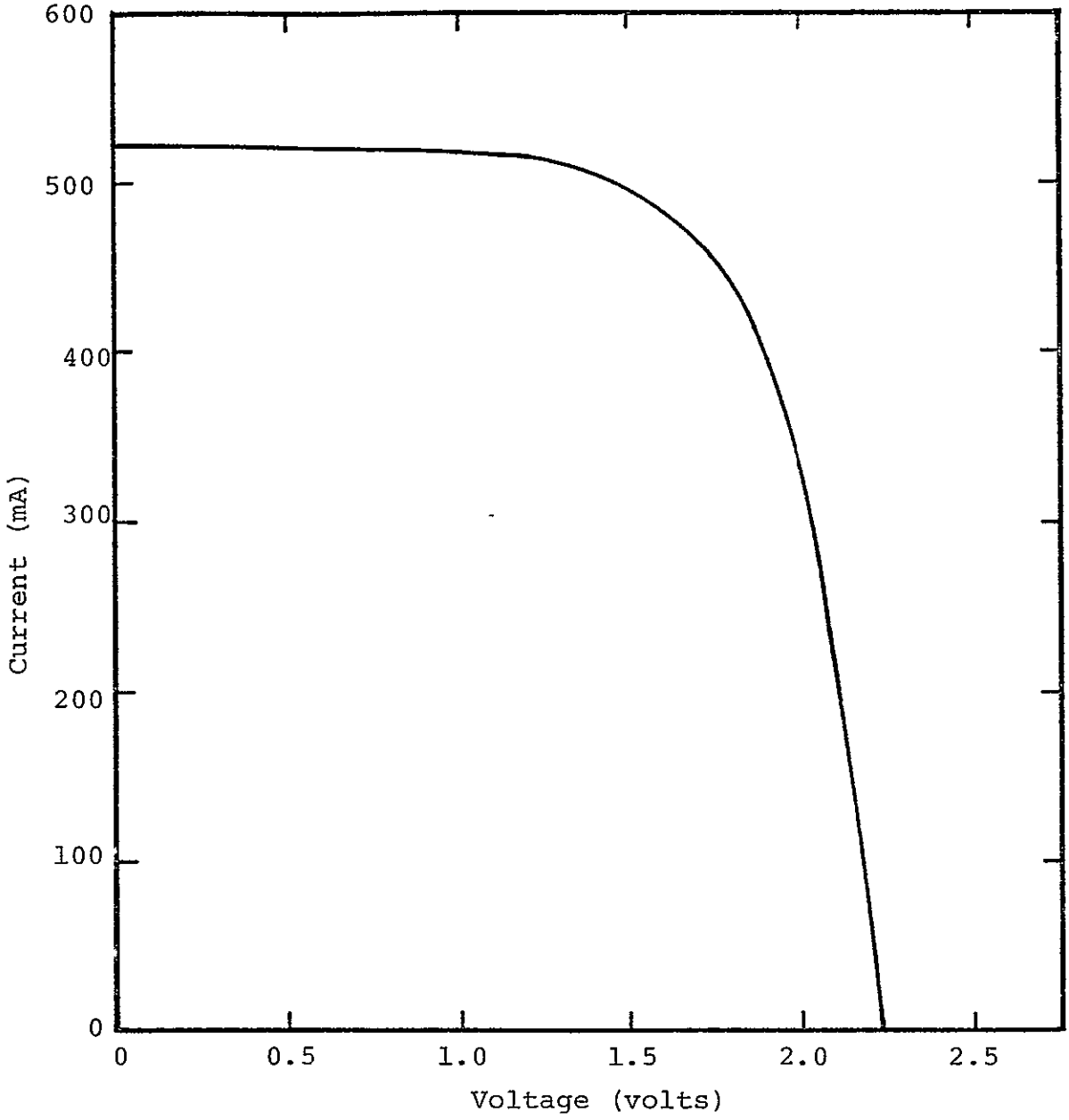


Figure 17. AMO I-V Curve of Four Cell Electrostatically Bonded Module, M1009

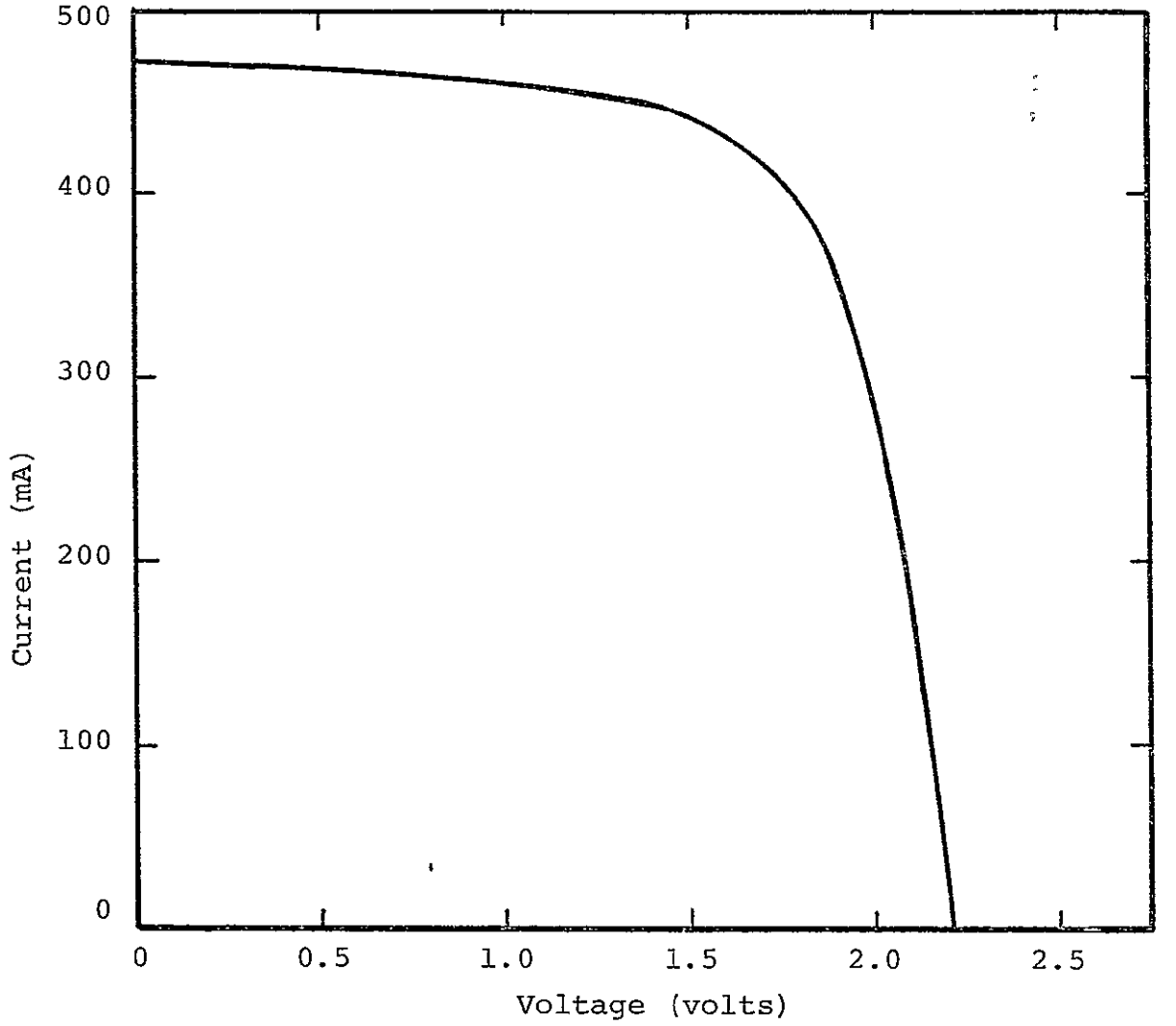


Figure 18. AMO I-V Curve of Four Cell Electrostatically Bonded Module, M1013

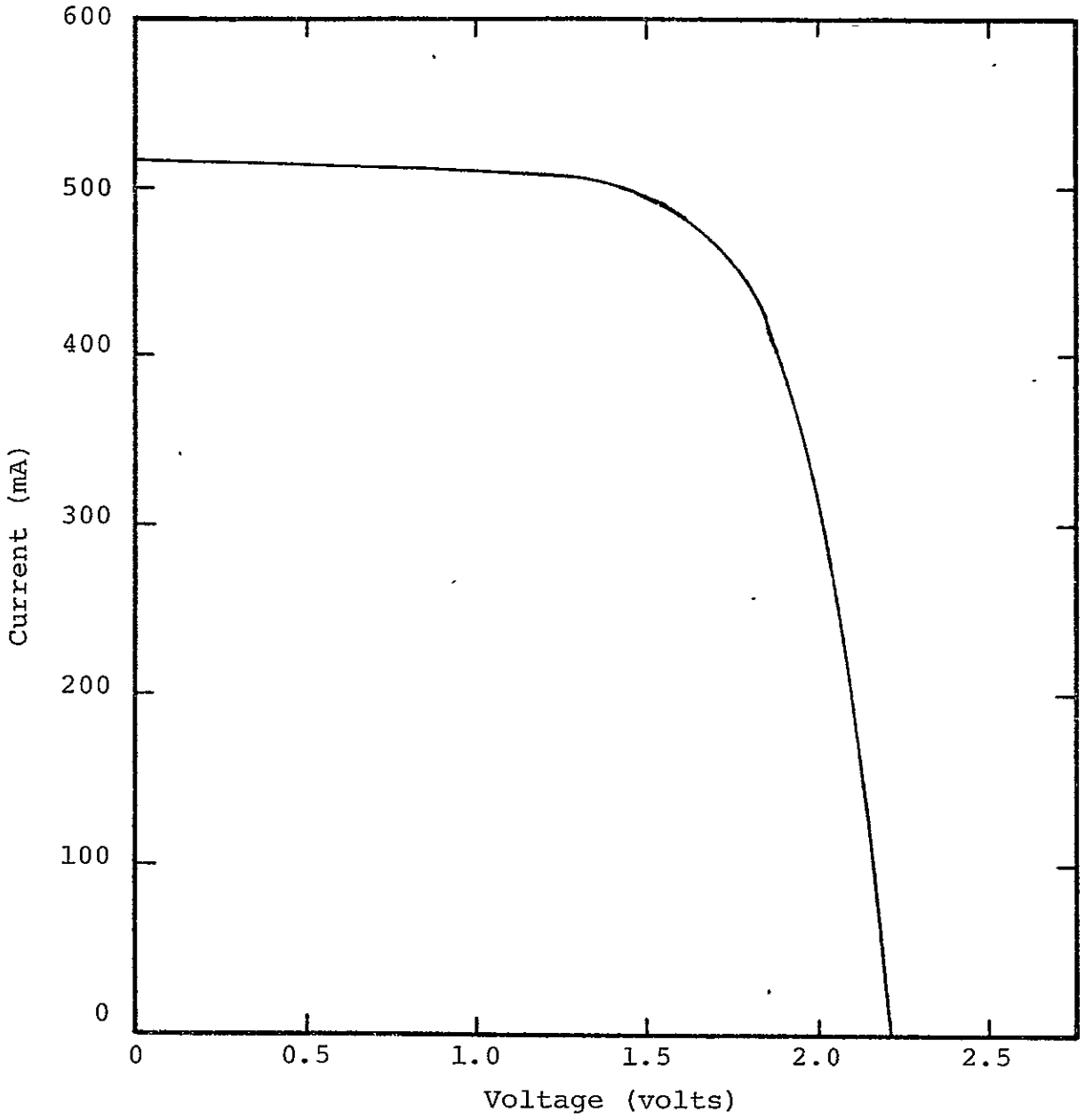


Figure 19. AMO I-V Curve of Four Cell Electrostatically Bonded Module, M1014

TABLE V

Summary of Type I Modules Delivered to JPL

| Module Number | M1008 | M1009 | M1013 | M1014 |
|---|---|---|---|---|
| Type | 4 Cell Series | 4 Cell Series | 4 Cell Series | 4 Cell Series |
| Metallization | Ti/Ag | Ti/Ag | Ti/Ag | Ti/Ag |
| Interconnects | Soldered Ag Mesh | Soldered Ag Mesh | Soldered Ag Mesh | Soldered Ag Mesh |
| Backing | RTV-11 W/SS4044 Primer | Polyroof | RTV-11 W/SS4044 Primer | Polyroof |
| Output Terminations | Binding Posts | Binding Posts | Binding Posts | Binding Posts |
| Anti-reflective Coating | $Ta_2O_5$ | $Ta_2O_5$ | $Ta_2O_5$ | $Ta_2O_5$ |
| $V_{oc}$ (volts) | 2.25 | 2.23 | 2.20 | 2.22 |
| $I_{sc}$ (mA) | 520 | 522 | 473 | 516 |
| Pmax (Watts) | 0.84 | 0.80 | 0.71 | 0.80 |
| Curve Factor | 0.72 | 0.68 | 0.68 | 0.69 |

TABLE VI

Electrical Properties of Module M1008
Before and After Electrostatic Bonding

| | Sample | Voc (V) | Isc (A) | Pmax (watts) | Fill Factor |
|---|---|---|---|---|---|
| Before Bonding | Cell 573-6 | 0.552 | 0.563 | 0.228 | 0.73 |
| | Cell 573-5 | 0.565 | 0.588 | 0.244 | 0.73 |
| | Cell 573-3 | 0.568 | 0.586 | 0.233 | 0.70 |
| | Cell 573-2 | 0.563 | 0.587 | 0.248 | 0.75 |
| | Totals | 2.248 | 2.324 | 0.953 | - |
| | Average | 0.562 | 0.581 | 0.238 | 0.728 |
| After Bonding | M1008 | 2.190 | 0.528 | 0.832 | 0.72 |

glass, more advanced module designs were made. The Type II module incorporates total glass sealing and elminates evaporated films on the glass. This design incorporates many of the bonding techniques developed throughout this program.

As with Type I, this module, shown in Figure 20, consists of four cells connected in series. Interconnection is by welded silver ribbons extending from the front of one cell to the rear of the next. The one mil thick ribbon, added to the height of the existing cell contact metallization, presented a difficult deformation bonding problem. If the bonding electrodes were not gently closed upon the sample, the cell would break along the central contact bar.

The bare ribbon caused shunting of the cell where it passed across the cell edge. This time the problem was solved by inserting a thin (0.001 inch) piece of amber mica (phlogopite) between the cell and the ribbon. With this insulation shunting has been no problem.

Joining of the interconnection ribbon to the cell backs was first done during bonding with a low melting point silver solder. This method was adequate but proved difficult because attempts to limit the heat input to the cell sometimes resulted in poor solder connections. A parallel gap welder was obtained and has eliminated the silver soldering of interconnections.

A shallow recess was machined in the back glass to accomodate the cells and interconnections. Machining of glass is not a practical production sequence but plastic deformation of the glass during rolling should be straightforward.

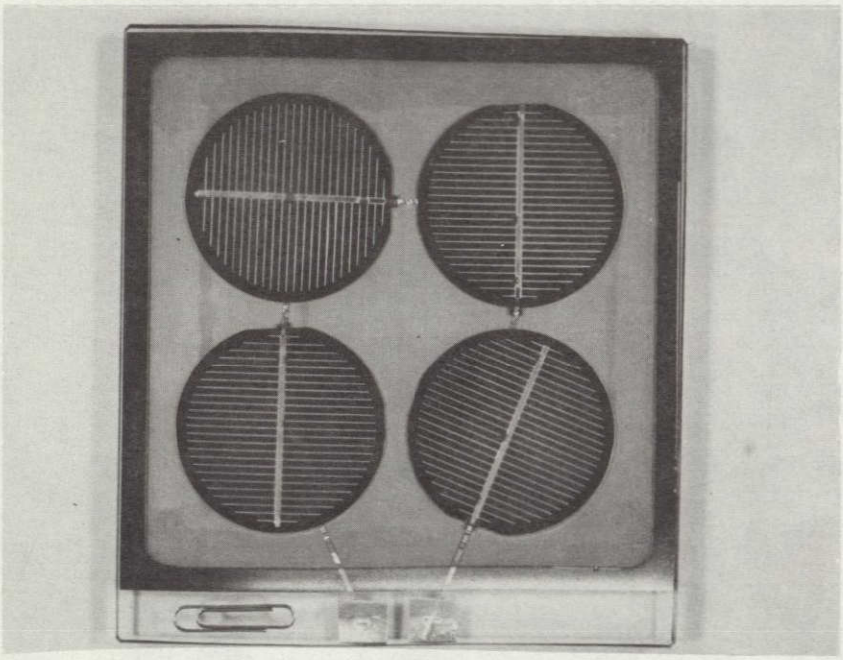

Figure 20. Four Cell Module with Total Glass Encapsulation

This recessed back glass does demonstrate total glass sealing and incorporates the glass to glass bonding techniques developed during this program. An interfacial layer of silicon was evaporated onto the glass back. Adhesion of this evaporated layer was assured by electrostatically bonding the film to the glass before attaching the glass to the module front. A second bond joined the two glasses.

Output leads were fed between the glass sheets. These leads terminated at a pair of bonded aluminum foil pads attached to the back surface of an extension of the front glass. The ribbons were attached to the bonded foils, originally by soldering but later by welding. Holes drilled through the glass and foils allowed attachment of threaded studs for electrical connections. The I-V characteristic of the first of these modules is given in Figure 21 and Table VII compares the pre-bond cell parameters to those of the completed module. Four of those modules will be delivered during Phase II of this program.

The design of a third module series has been completed and one cell versions have been fabricated. This totally integral design is similar to the Type II except that the back glass is not preformed. Ideally, this module would be fabricated in one step in which two sheets of glass are deformed around the cells during bonding.

To date mechanical limitations of the bonding facility have prevented one step fabrication. The bonding electrodes cannot be closed upon the sample without

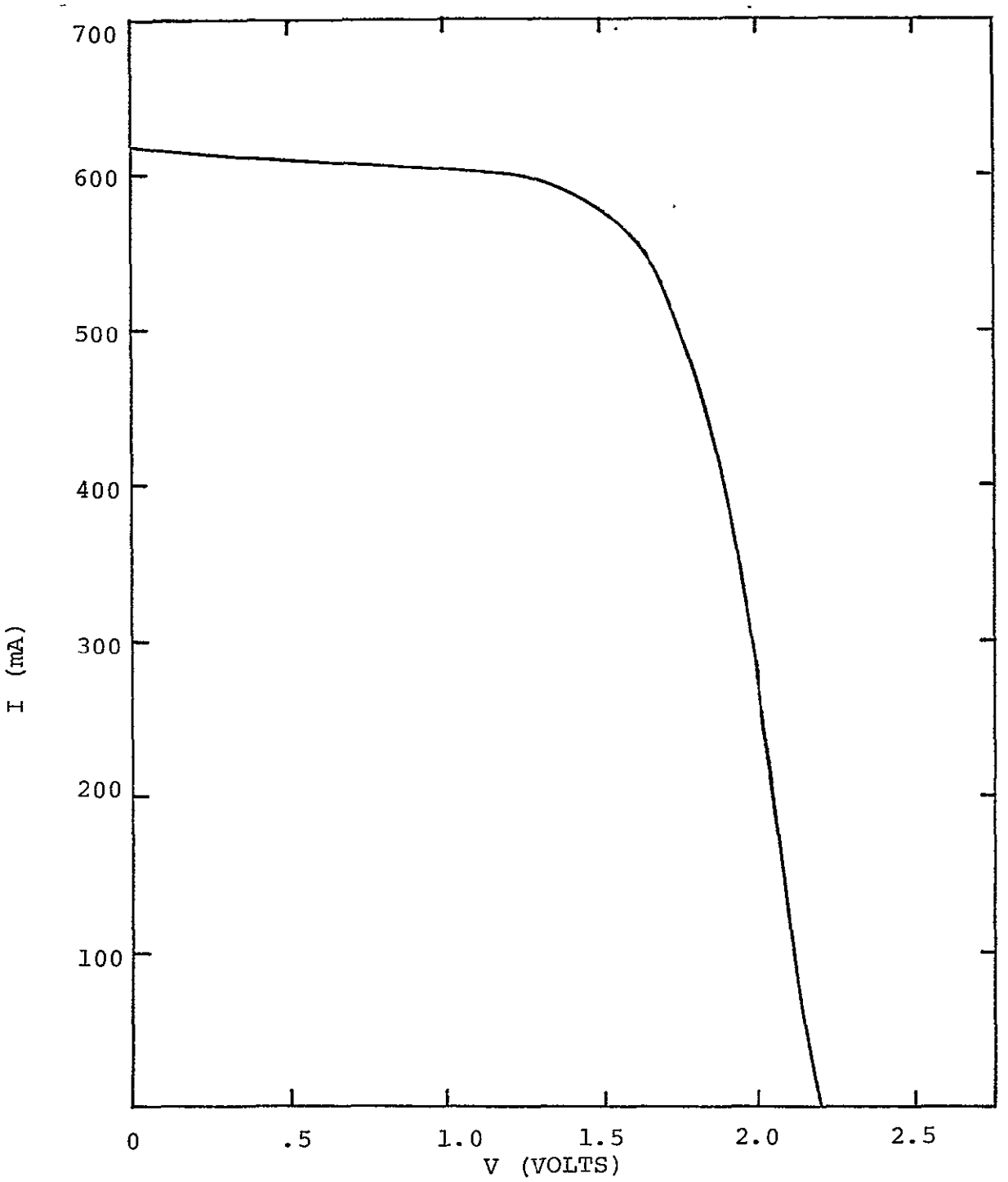


Figure 21. Four Cell Total Glass Encapsulated Type II Module

TABLE VII

Characteristics of Four Cell, Type II Module Before and After Bonding

| | Sample | $V_{oc}$ (V) | $I_{sc}$ (A) | $P_{max}$ (Watts) | Fill Factor |
|---|---|---|---|---|---|
| Before Bond | Cell 890-7 | 0.56 | 0.69 | 0.23 | .59 |
| | Cell 890-9 | 0.56 | 0.69 | 0.24 | .62 |
| | Cell 890-10 | 0.56 | 0.67 | 0.26 | .69 |
| | Cell 890-11 | 0.56 | 0.69 | 0.26 | .67 |
| | Totals | 2.24 | 2.74 | 0.99 | - |
| | Averages | 0.56 | 0.68 | 0.25 | .64 |
| After Bond | M2001 | 2.20 | 0.63 | 0.95 | .69 |

breakage, unless both sheets of glass are at high temperature. Since it has not been possible to properly preheat the glass, modules of this type must be made in two steps. Multiple cell modules of this type should be made early in Phase II of this program if no major obstacles are encountered in the scale up from the single cell configuration.

Two of the integral front, Type I, modules underwent thermal cycling and humidity \testing at JPL. Standard LSSA module acceptance testing procedures, as shown in Figures 22 and 23, were used. Thermal tests consisted of fifty (50) cycles between -40° C and +90° C at a maximum rate of 100°C/hr. Humidity testing involved pre-dry and humidity soak cycles followed by five days at 90-95% relative humidity at 40°C. The evaporated film metallization on the glass showed signs of slight attack, probably due to moisture penetration through the modules' organic back coatings. However, there was no evidence of any effect upon the electrostatic bonds. There was no degradation in module performance. Electrical output of both modules was unchanged from the pre-test values.

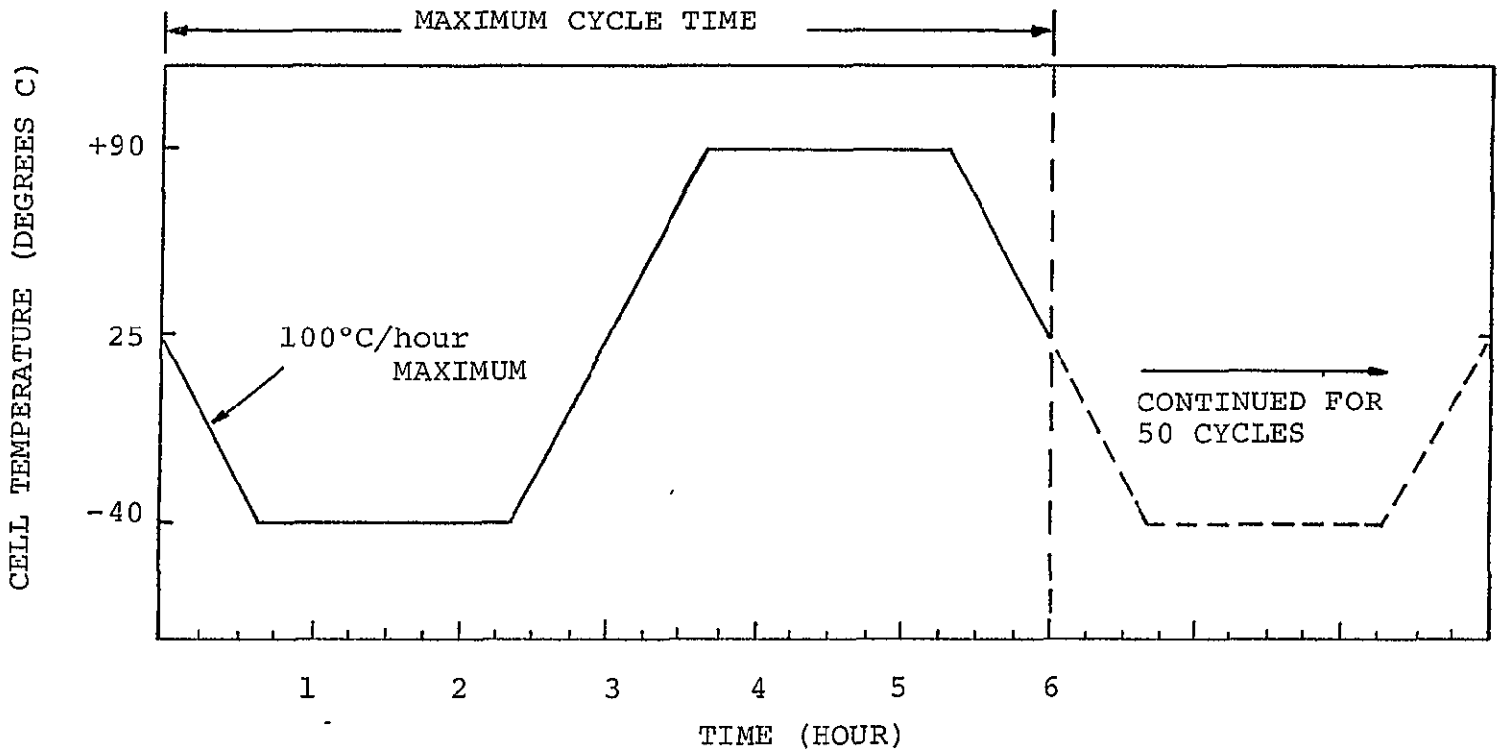


Figure 22. Standard LSSA Thermal Cycle Test Used on Electrostatically Bonded Demonstration Modules

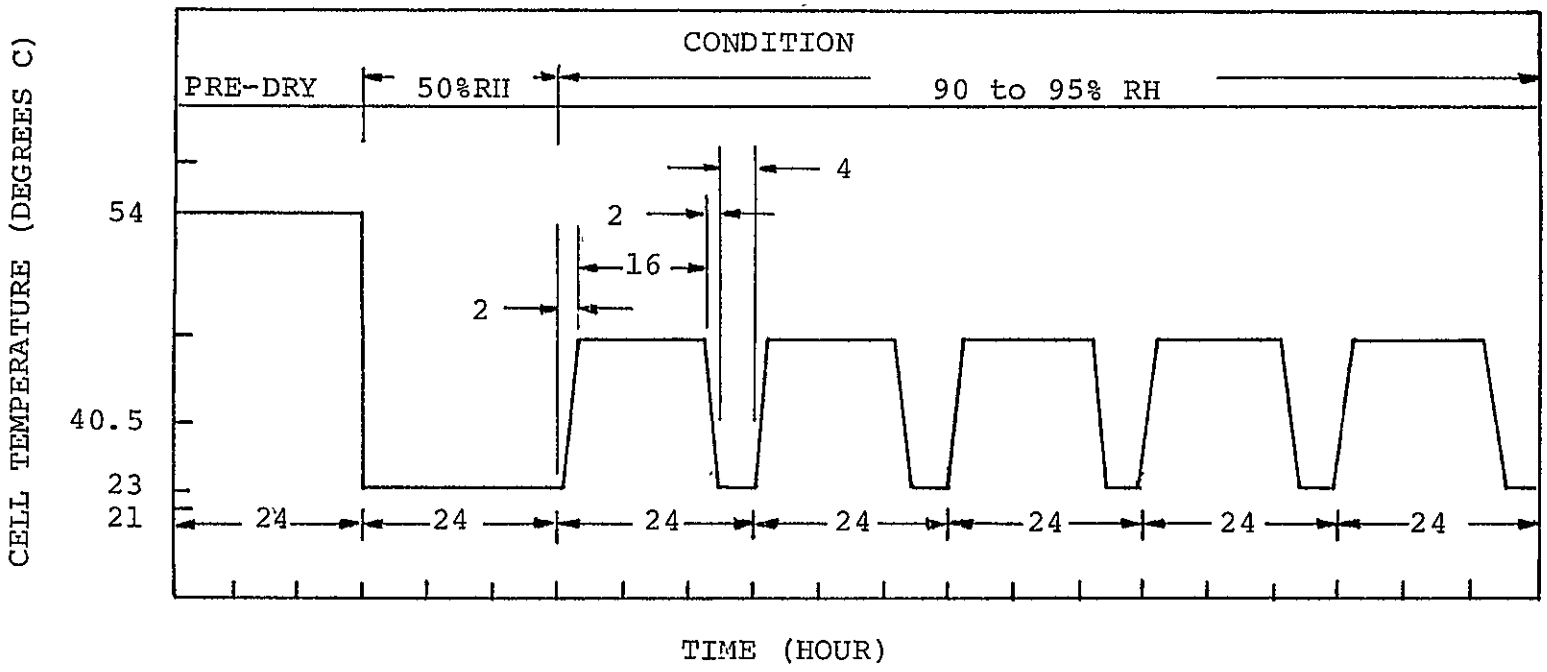


Figure 23. Standard LSSA Humidity Cycle Test Used on Electrostatically Bonded Demonstration Modules

## 5.0 CONCLUSIONS

This program has assessed and developed electrostatic bonding for integral glass encapsulation of terrestrial solar cells. Processes that can be fast, reproducible, and inexpensive have been developed. Excellent stability of electrostatic bonds has been demonstrated.

Early in this program a first large area electrostatic bonder was built. Subsequently, a second large area bonder with controlled environment was designed and fabricated. With these facilities existing electrostatic bonding technology was adapted to terrestrial solar cells. The technology was extended to cover a number of problems peculiar to terrestrial applications.

During this program the first large area electrostatic bonds were formed. Bonding of multiple cell configurations was achieved. Techniques for major deformation bonding were established. Routine bonding to cells with thick contact metallization can now be accomplished without degradation of cell electrical performance.

Glass materials for terrestrial modules have been selected with primary emphasis on matching the thermal expansion of silicon. Requirements on the glass surface condition have been established. While irregular surfaces can be bonded to and polished surfaces are ideal, the intermediate quality of rolled glass is more than adequate.

An extended range of bondable materials was identified during this program. These include a variety of metals and dielectrics in evaporated film form plus metal foil and screen printed inks. Bonding of several materials was made possible by use of a controlled environment. Preliminary assessment of the effects of various bonding atmospheres was carried out.

Quantitive measurements of bond quality were made for the first time. Establishment of a lap shear test capability demonstrated the electrostatic bonds formed with many materials are stronger than the glass to which these materials are joined. A preliminary configuration for testing the hermeticity of electrostatic bonds was developed.

The technology developed under Phase I of this program has been combined to yield functioning multiple cell modules. These modules include cells bonded to glass sheets without loss of electrical performance. Interconnection techniques have been developed to join the cells either in series or parallel. Glass to glass bonding with interfacial films has been used to produce total glass encapsulation of solar cells.

This electrostatic bonding development program has been successful. A promising technique for solar cell encapsulation has been identified and shown to be practical. This process should yield an encapsulation system that should meet or exceed LSSA 20 year lifetime goal.

Development efforts will continue under Phase II. Facility modification will provide programmed control of bonding operations. This control will allow a thorough and systematic examination of the bonding process. Combined with an analysis of the physics of the bonding mechanism, this study should fully characterize electrostatic bonding. Development of practical module configurations will continue with emphasis on cost effective methods and advanced bonding techniques.

## APPENDIX I

### Properties of Candidate Glasses for Electrostatic Bonding

Figures 24 and 25 show the thermal expansion and viscosity of glasses considered for electrostatic bonding. Comparision to silicon shows that 7070 has the best expansion match. Samples bonded to 7070 at a temperature of 490°C would show the zero residual stress when returned to room temprature.

Figure 26 shows the optical transmittance of 7070 glass over the operating band of silicon solar cells. The spectral response of a typical cell is shown in Figure 27.

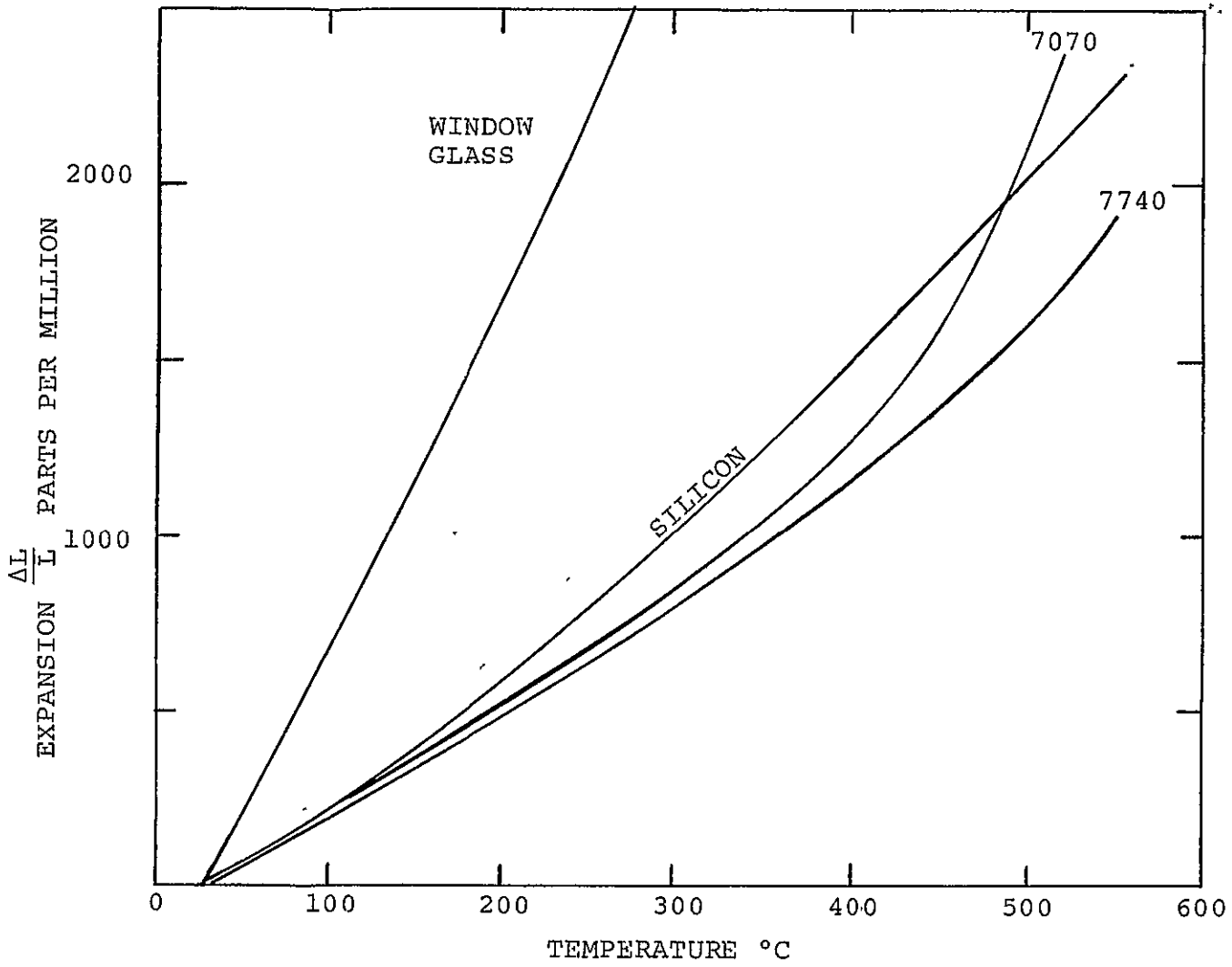


Figure 24. Thermal Expansion Characteristics of Glass Material Compared to Silicon

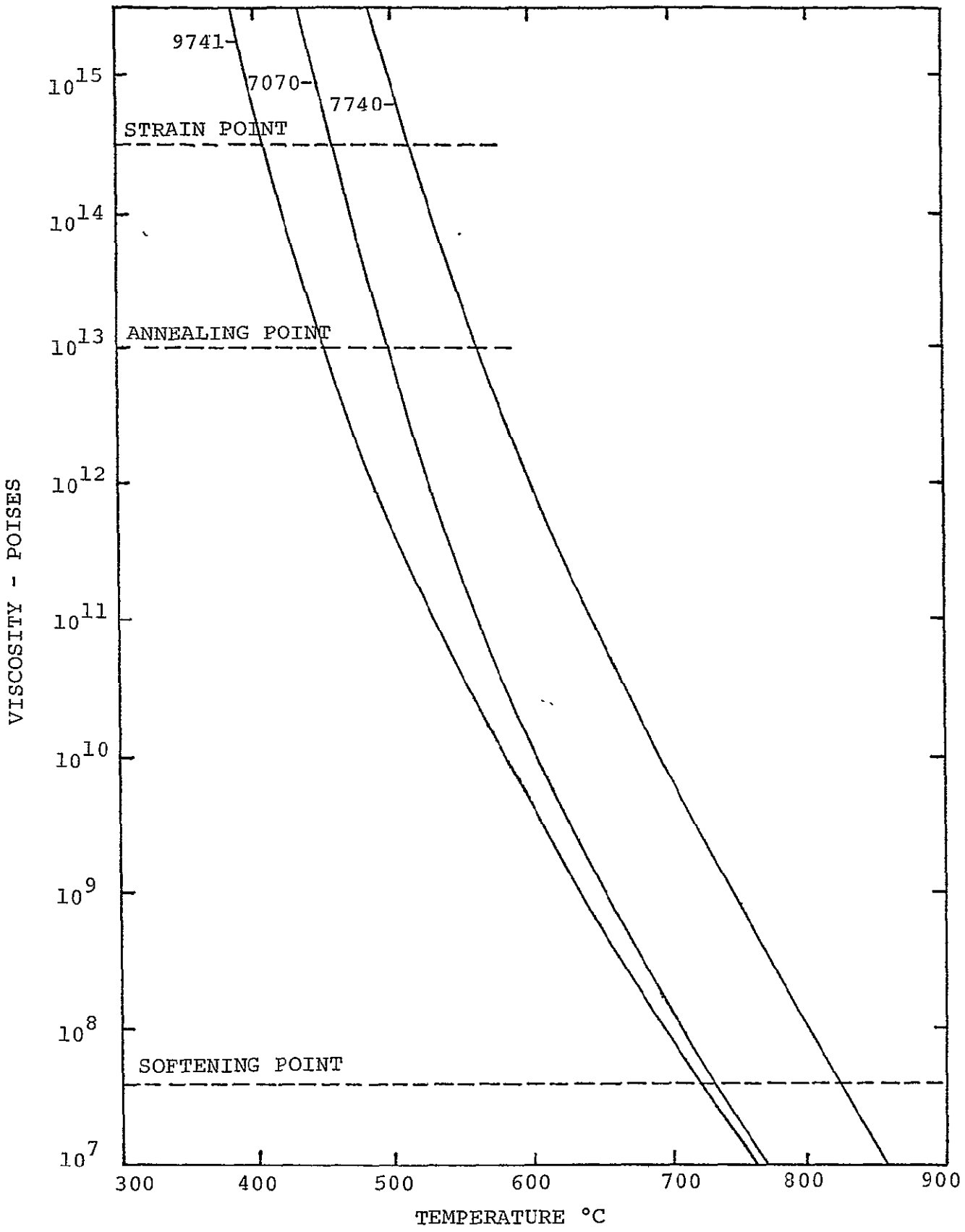


Figure 25. Viscosity versus Temperature for 7740, 7070, and 9741 Glasses

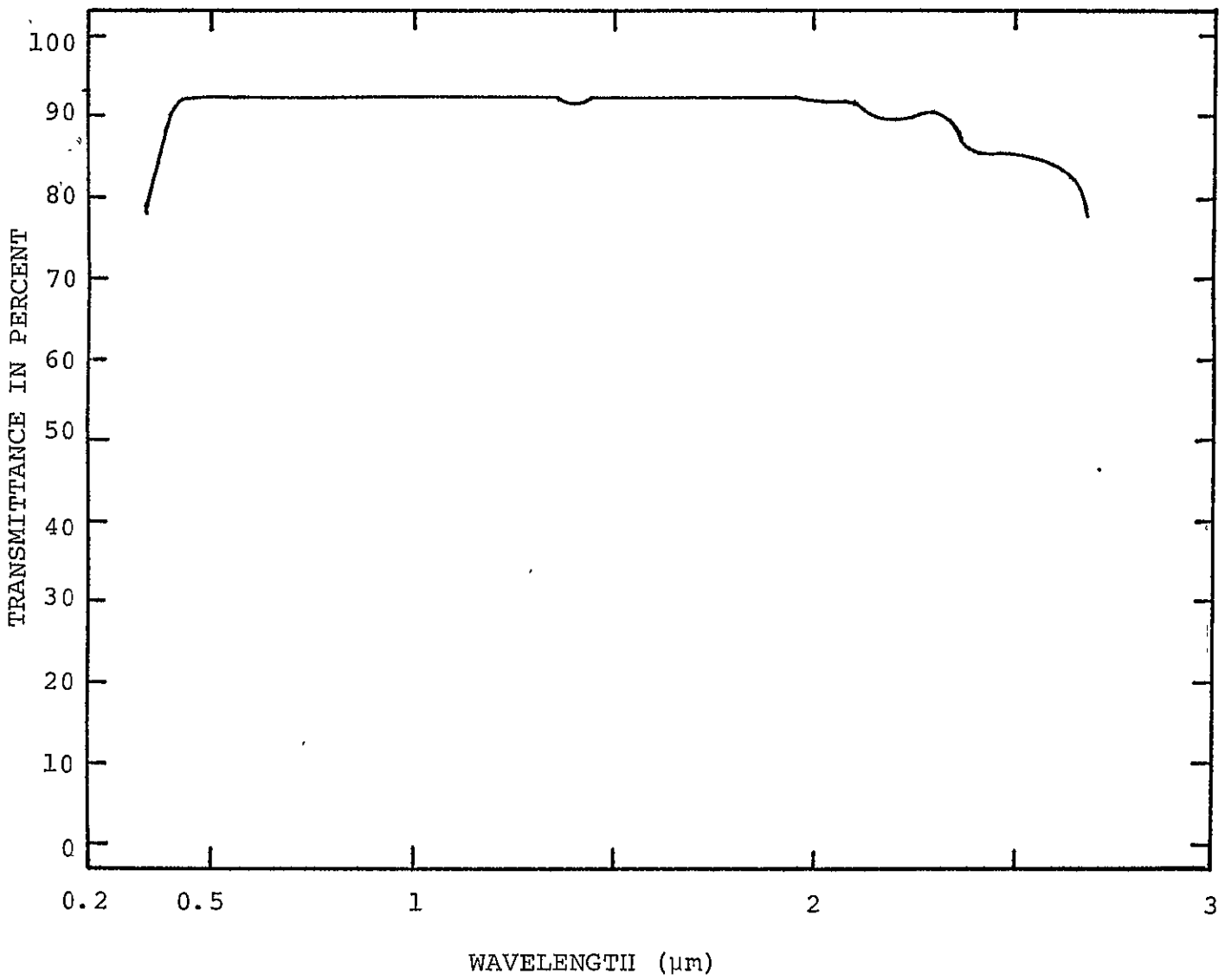


Figure 26. Transmittance of 7070 Glass

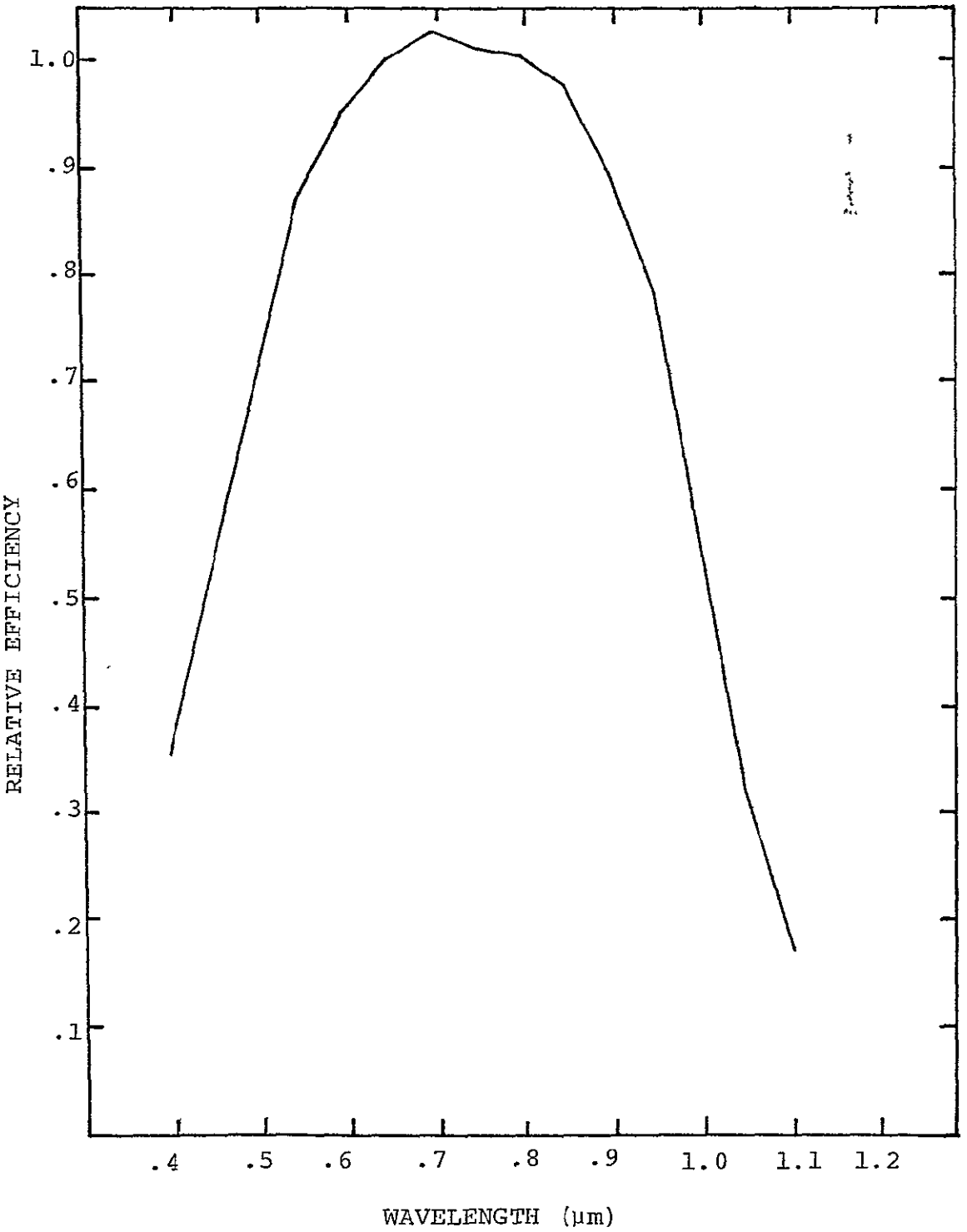


Figure 27. Relative Quantum Efficiency of Implanted Silicon Solar Cell

## APPENDIX II

## Stresses In Bonded Silicon-Glass Assemblies

The stresses that exist in cylindrical configurations of glass and metal (semiconductors) are axial (longitudinal), radial, and circumferential (tangential). These stresses may be either compression stresses or tension stresses and they result from the different overall expansions of the two elements that make up the bonded assembly.

A simple, one dimensional example can illustrate how stresses originate in bonded assemblies and how the stresses may be calculated. Consider long narrow strips of Pyrex glass and silicon. Assume that these strips, when heated to a bonding temperature of about 500°C, have exactly the same length. We know from the expansion curves of Pyrex glass and silicon (See Figure 24) that silicon expands more than Pyrex over the temperature range from room temperature, say 27°C to 500°C. In fact, this graph shows that silicon expands about 420 ppm ($420 \times 10^{-6}$) more over this temperature range. Thus if the strips of Pyrex and silicon were allowed to cool down to room temperature without bonding, the Pyrex strip would be shorter by the fractional amount of $420 \times 10^{-6}$. On the other hand, if one first bonded the strips at the temperature of 500°C and then allowed them to cool down to room temperature, it would be found that the final length of the composite assembly was some value between the two lengths of the unjoined cold materials. That is, the silicon, which wanted to contract more, is not allowed to do this by the Pyrex, and thus its final length is longer than its free, cold length. The process has put

the silicon into tension. On the other hand, the Pyrex is made to contract more than it would if it were free, and so the Pyrex is put into compression.

Now we know from the definition of the elastic modulus E of any solid that

$$E = \frac{\text{stress}}{\text{strain}} = \frac{\text{Force/area}}{\text{change in length/length}}$$

The total fractional change in length of the two strips discussed above over the temperature range of 27°C to 500°C is:

$$\frac{\Delta \ell}{\ell} = \frac{\Delta \ell_2}{\ell_2} - \frac{\Delta \ell_1}{\ell_1} = (\alpha_2 - \alpha_1)\, \Delta T = -420 \times 10^{-6}$$

where $\alpha_2$ and $\alpha_1$ are the thermal expansion coefficients of the Pyrex and silicon respectively, $\Delta T$ is the temperature range (500°C - 27°C), $\Delta \ell_2/\ell_2$ and $\Delta \ell_1/\ell_1$ are the fractional changes in length of the Pyrex and silicon over the temperature range.

If the elastic moduli of the silicon and Pyrex glass were equal, then the final length of the bonded silicon-Pyrex assembly would be exactly halfway between the two free cold lengths of the silicon and Pyrex strips. This means that the actual strain (fractional change in length) is one half of the total strain given above, or

$$\text{Stress} = \text{Strain} \times E = \frac{\alpha_2 - \alpha_1\, \Delta T}{2} \times E$$

If the elastic modulus E above is taken to be an average of the two moduli, the equation above is a reasonable approximation for most types of seals.

More exact derivations of the stress between two flat bonded plates yield the equation:

$$\text{stress} = \rho = \frac{(\alpha_2 - \alpha_1)\ \Delta T\ E_1\ E_2}{(\sigma - 1)(E_1 + E_2)}$$

where $\sigma$ is Poisson's ratio and accounts for the change in cross section as a plate is either stretched or compressed, and $E_1$ and $E_2$ are the moduli of the two bonded pieces.

A few numerical examples will be given next to illustrate the use of the stress equation. From expansion curves of silicon and Pyrex over the temperature range from room temperature to 500°C, the differential expansion is about -420 ppm or $-420 \times 10^{-6}$.

The theoretical value of the stress becomes:

$$P_{\text{Si-Pyrex}} = \frac{\delta\ E_1\ E_2}{(\sigma - 1)(E_1 + E_2)}$$

where

$$\delta = (\alpha_2 - \alpha_1)\ \Delta T = \frac{\Delta \ell_2}{\ell_2} - \frac{\Delta \ell_1}{\ell_1} = -420 \times 10^{-6}$$

$$E_1 = 2.75 \times 10^7 \text{ psi for silicon}$$
$$E_2 = 0.95 \times 10^7 \text{ psi for Pyrex}$$
$$\sigma = .20 \text{ for Pyrex}$$

Then

$$P_{Si\text{-}Pyrex} = \frac{-420 \times 10^6 \times 2.75 \times 10^7 \times 0.95 \times 10^7}{(.20 - 1)\ [2.75 \times 10^7 \times 0.95 \times 10^7]}$$

or $$P \simeq 3{,}700 \text{ psi}$$

This stress is positive and is thus compressive in the glass in the region where the silicon wafer is bonded. The radial compressive stress at the circular boundry between the bond region and the free glass pulls the free glass inward and puts it into radial tension with maximum tensile stress of 3,700 psi at the circumferential interface between the free glass and the edge of the circular bonded region. The tangential stress at this interface is compressive so the free glass should only break along the edge of the bonded region as a result of the radial tension. A stress of 3,700 psi is outside the safe working stress range for untempered glass.

The radial stress diminishes with increasing radius r from the circumference $r_1$ of the bonded region to the outermost radius $r_2$ in accord with the Lamé equations:

$$\text{Radial stress} = P_x \frac{r_1^2}{r_2^2 - r_1^2} \left(1 - \frac{r_2^2}{r^2}\right)$$

## REFERENCES


(1) Carmichael, D. C., et al, "Review of World Experience and Properties of Materials for Encapsulation of Terrestrial Photovoltaic Arrays", Final Report ERDA/JPL Contract 954328, Battelle, 1976.

(2) NASA Contract NAS5-21510, Heliotek.

(3) Air Force Contract F33615-68-C-1198, Heliotek.

(4) Air Force Contract F33615-70-C-1619, Heliotek.

(5) NASA Contract NAS5-10319, Texas Instrumnts

(6) ESRO Contract 810/69/AA, Electrical Research Association.

(7) ESRO Contract 1407/71/AA, Electrical Research Association.

(8) NASA Contract NAS5-10236, Ion Physics Corporation.

(9) Air Force Contract F33615-67-C-1158, Ion Physics Corporation.

(10) NASA Contract NAS5-3857, Hoffman Electronics.

(11) Air Fore Contract F33615-70-C-1656, General Electric.

(12) Kirkpatrick, AR, Kreisman, W. S. and Minnucci J. A., "Stress Free Application of Glass Covers for Radiation Hardened Solar Cells and Arrays", Final Report, Air Force Aero Propulsion Laboratory Contract F33615-74-C-2001, Simulation Physics, (now Spire Corporation) 1977.

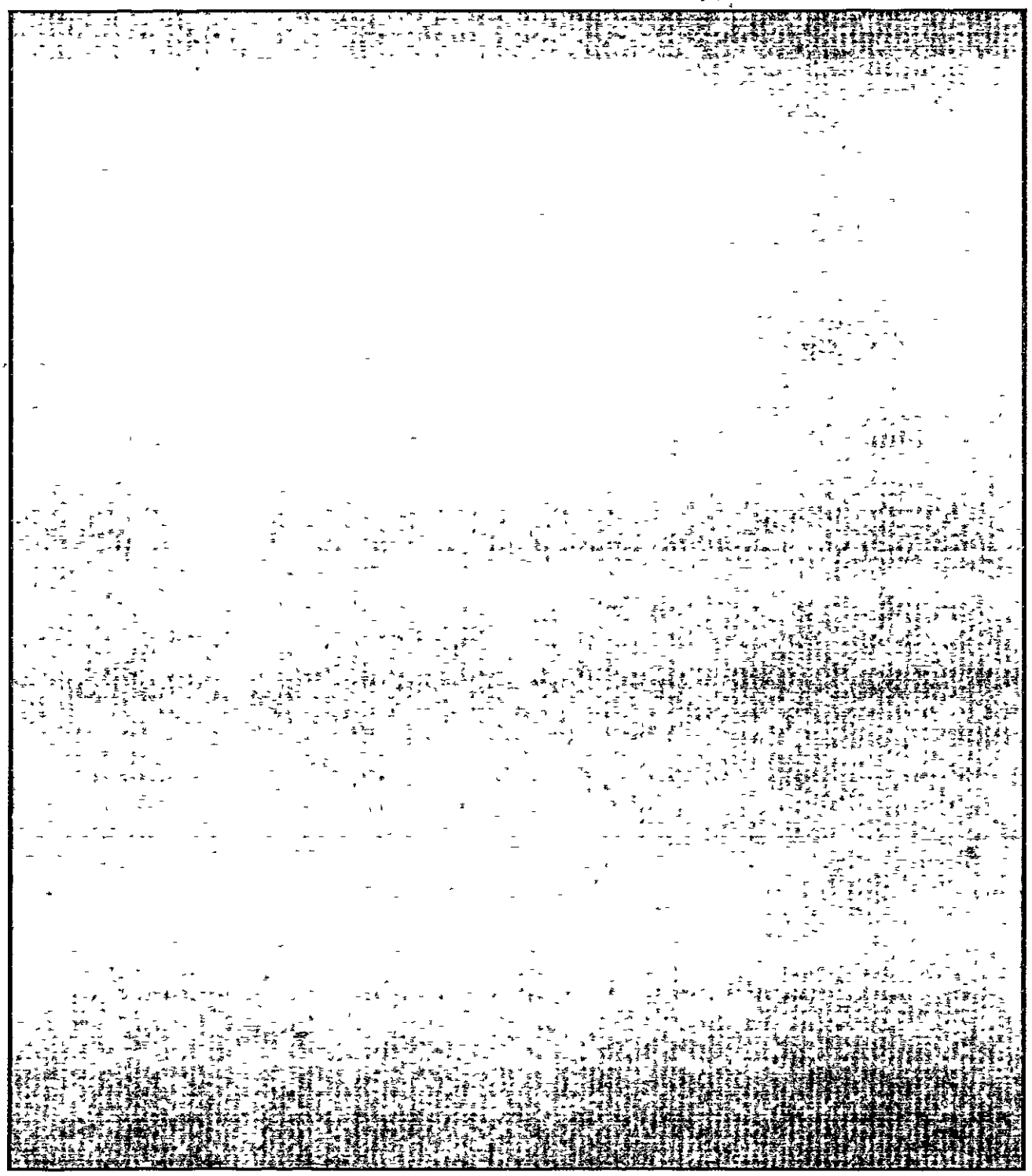

spire
CORPORATION

PATRIOTS PARK / BEDFORD, MASSACHUSETTS 01730

Formerly Simulation Physics, Inc